POLITECNICO DI MILANO

School of Industrial and Information Engineering

Department of Physics

Master Thesis in
Engineering Physics

Fano resonances in optical waveguide lattices

Supervisor:
Prof. Stefano LONGHI

Candidate:
Fabrizio SANTIN
Matr.787141

Academic Year 2017 - 2018

Politecnico di Milano:
www.polimi.it

School of Industrial and Information Engineering:
www.ingindinf.polimi.it/en/

Acknowledgments

I would like to thank Prof. Longhi, supervisor and proponent of this Master Thesis, for the availability and precision shown to me during the final drafting period.

I would also like to thank Prof. Gianluca Valentini and Dott.ssa Dafne Forloni, who guided me with extreme kindness through the process of finding a supervisor.

Milano, April 2019

Contents

List of Figures

Abstract

In this dissertation we discuss the occurrence of Fano resonances and bound states in the continuum in arrays of evanescently coupled dielectric optical waveguides. We will focus on Fano resonances in static photonic structures, their role in analyzing particle statistics and in non-Hermitian optical structures.

Sommario

In questo elaborato discutiamo la comparsa di risonanze di Fano e stati legati nel continuo in allineamenti di guide d'onda dielettriche in accoppiamento evanescente. Ci focalizzeremo su risonanze di Fano in strutture fotoniche statiche, il loro ruolo nell'analizzare la statistica di particelle e su strutture ottiche non Hermitiane.

Introduction

One of the most important phenomena in physics is resonance.
In mechanical system that can perform, in the absence of damping, free oscillations at a particular frequency ω_0, if we apply to the system a driving force with a frequency ω, this force will induce a large response in the system when the frequency ω is close to ω_0, providing that the damping is not too large [1]. Frequencies at which the response amplitude is a relative maximum are known as resonance frequencies of the system. In other systems phenomena occur which are described as resonance but depend on interaction between different aspects of the system, not on an external driver. The phenomenon of resonance is a general physical principle that applies everywhere and at every level, from classical to quantum mechanical systems.

Resonances are both feared and sought after. Engineers, assembling bridges and raising high buildings, subject to wind pressure and periodic stress, do their best to suppress resonances, which, if not carefully taken into consideration, may bring those structures to a catastrophic end. A nuclear reactor is designed around the absorption resonances that a neutron on its way from high energies, when born in the fission of uranium, down to thermal energy, has to avoid, before being useful again in the chain reaction. Optical fibers, used to transport light signals, are designed to work in a particular frequency window, in order to minimize absorption and increase efficiency.

A fundamental field in which resonances played a crucial role in the history of mankind was absorption of radiation by atoms. Absorption lines were observed in transitions between bound levels of hydrogen in the interaction with radiation, at the end of the 19th century, later allowing Niels Bohr to deduce his model of the atom, which laid the basis of quantum mechanics. The typical shape of the response curve of these resonances is that of a Lorentzian function, which is symmetric and centered at the resonant frequency. These are called Breit-Wigner resonances.

However, not all resonances shared these features. Another kind of lineshape emerged, above the ionization energy, in the continuum, for some noble gases. A lineshape that was asymmetric and had no explanation. The first to describe these spectral atomic profiles was Ugo Fano in 1935 [2], a young postdoctoral fellow in the group of Enrico Fermi, and later, in 1961 [3], in a much more refined work. He gave an interpretation of these "strange-looking shapes" based on the quantum mechanical principle of superposition and interference between discrete excited states and the continuum, sharing the same energy. This second paper by Fano became one of the most important publications in the physics of the 20th century. Together with an asymmetric shape, Fano resonances may come with another interesting feature: destructive interference. Usually, as already discussed, reso-

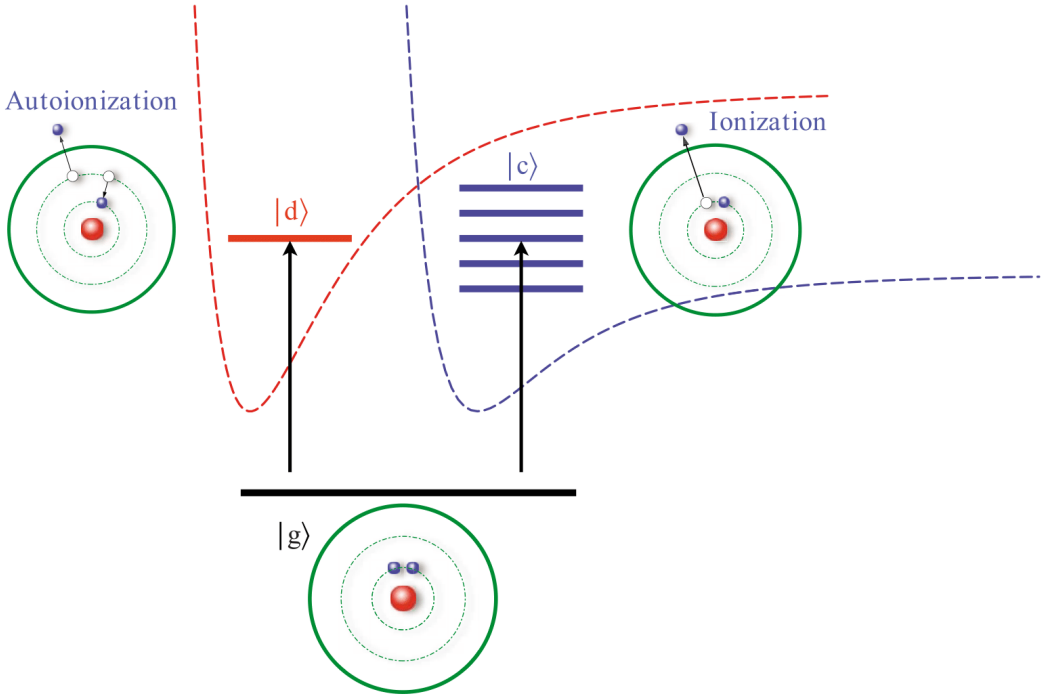

Figure 1: Fano resonance as a quantum interference of two processes: direct ionization of a deep inner-shell electron and autoionization of two excited electrons followed by the Auger effect. This process can be represented as a transition from the ground state $|g\rangle$ of an atom either to a discrete excited autoionizing state $|d\rangle$ or to a continuum $|c\rangle$. Dashed lines indicate double excitations and ionization potentials. [18].

nances enhance the response of a system, for better or worse. On the contrary, a Fano resonance, sometimes called an "antiresonance" may slow down the system, partially or completely, suppressing its dynamics. Two simple examples are given to elucidate these two characteristics of Fano resonances. First we consider light interacting with an atom [18]; see Figure 1. A photon of frequency ν interacts with the atom, which can emit an electron in a process called photoionization. There are many ways in which this can happen. The simplest one is the excitation of an inner-shell electron above the ionization threshold, $A + \hbar\nu \rightarrow A^+ + e^-$ (Figure 1 (right)). In this process the whole atom, when coupled to the radiation field, goes to an energy level in the continuum and then emits the electron into the continuum at that energy. Another process is the excitation of the whole atom to a quasidiscrete state, in our case two electrons excited from an inner-shell to a higher shell, followed by the relaxation of one electron transferring its energy to the another one, thus being emitted, $A + \hbar\nu \rightarrow A^* \rightarrow A^+ + e^-$ (Figure 1 (left)). This process is called autoionization. The excited atom finds itself on a level, clearly a bound state, but above the first ionizing threshold, in the continuum. This process of autoionization can be considered to couple continuum states of one channel with bound states of another. Because of the superposition principle of quantum mechanics, whenever two states are coupled by different paths, interference may occur. And this is the idea Fano had in mind when he wrote his papers on this argument.

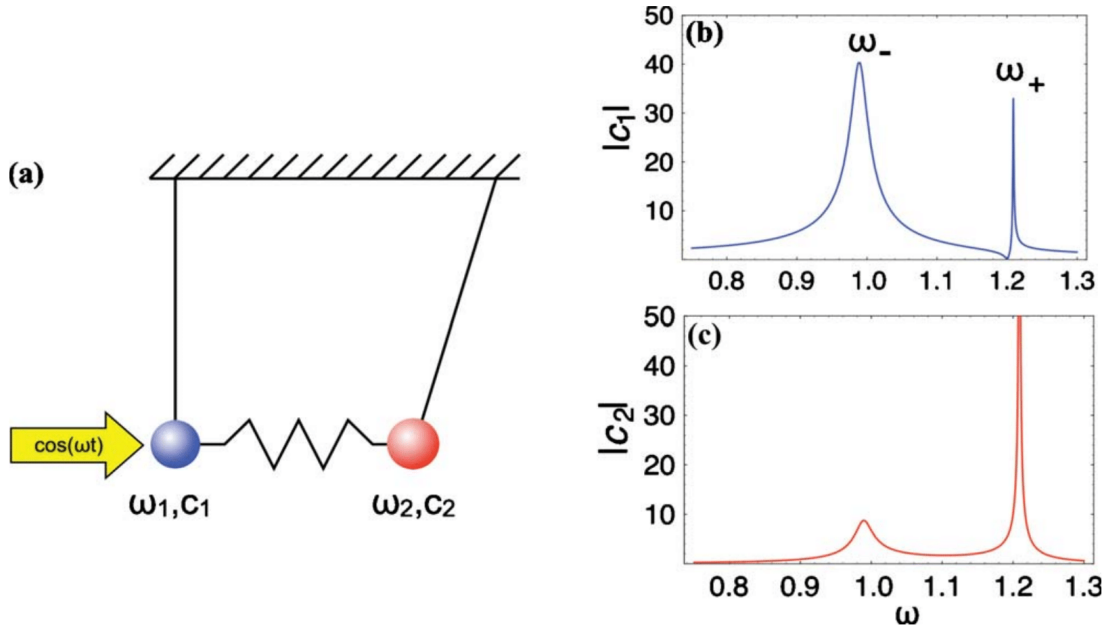

Figure 2: Resonances of parametrically driven coupled oscillators. (a) Schematic view of two coupled damped oscillators with a driving force applied to one of them; (b) amplitude of the forced oscillator $|c_1|$ versus frequency, and (c) amplitude of the coupled oscillator $|c_2|$ versus frequency. [18].

But, as already mentioned, Fano resonances are not limited to quantum mechanics. A relatively simple mechanical system, showing Fano resonance, is composed of two pendula coupled with a spring, with one of the oscillators driven by a periodic force of frequency ω_0; see Figure 2. The analysis of the system [19] shows that, near its eigenfrequencies ω_1 and ω_2, there are two resonance frequencies ω_- and ω_+ with different behaviors. As can be seen in Figure 2(b), the resonance at ω_- is an usual symmetric one, which amplifies the oscillation amplitude c_1 of the first pendulum. Something different happens at ω_+; the shape of the resonance is asymmetric and there's also a dip near it, actually going to zero. The oscillation amplitude of the first pendulum goes to zero! There is total destructive interference between the driving force and the influence of second oscillator, two channels that interfere. Nothing "strange" happens to the second pendulum, as seen in Figure 2(c), since there's only one channel.
Another important thing to notice is the narrowness of the Fano resonance, which will turn out to be extremely useful in sensor applications.

Just like their more popular counterparts, Fano resonances are ubiquitous and span many areas of physics. We will focus on their appearance in optical structures made up of waveguides.

Chapter 1

Building the optical structure

Our goal is to build an optical structure where Fano resonance and the rich seam of physics phenomena connected to it come into play. Having in mind the scattering experiments with noble gases that stimulated the young mind of Fano, we need to get hold of both discrete levels and the continuum and couple them together. The natural starting point is (non-relativistic) quantum mechanics, based on the Schrödinger equation:

$$i\hbar\frac{\partial}{\partial t}\left|\psi(t)\right\rangle = \frac{\hat{\mathbf{p}}^2}{2m}\left|\psi(t)\right\rangle + V(\hat{\mathbf{x}},t)\left|\psi(t)\right\rangle \tag{1.1}$$

which describes the time evolution of the state $|\psi(t)\rangle$ of a particle with mass m in a potential V. The state, everything we know about the particle, lives in an abstract Hilbert space, a complex vector space endowed with an inner product that makes it complete in the induced metric. Linear operators, indicated here with little hats on them, acts on these states. In the position representation, the state of the particle is the wave function $\psi(\mathbf{x},t) = \langle\mathbf{x}|\psi(t)\rangle$, a complex-valued function belonging to $\mathcal{L}^2(\mathbb{R}^3)$ over the variable $\mathbf{x}$; the momentum operator becomes $-i\hbar\boldsymbol{\nabla}$ and the position operator is simply multiplication by $\mathbf{x}$. The Schrödinger equation takes the following form

$$i\hbar\frac{\partial}{\partial t}\psi(\mathbf{x},t) = -\frac{\hbar^2}{2m}\nabla^2\psi(\mathbf{x},t) + V(\mathbf{x},t)\psi(\mathbf{x},t) \tag{1.2}$$

The meaning of the wave function, according to Born's rule, is that its square modulus, integrated over a volume, is the probability to find the particle in that volume, at time t.

An analogy with electromagnetism and the intensity of the electromagnetic field, can be drawn. Consider first a step-index, weakly guiding, single-mode at the operating wavelength, straight, infinite optical fiber, the only kind we will deal with. The core, of refractive index n_a, is circular with radius r and embedded in an infinite substrate of refractive index n_c. This will serve as the basic building block of the photonic structure.

A Cartesian orthogonal coordinate system $Oxyz$ is placed with the origin at the center of the core, with the z axis along the fiber. Unit vectors along the positive directions of the coordinate axes x, y and z, are indicated by $\mathbf{e}_x$, $\mathbf{e}_y$ and $\mathbf{e}_z$, respectively.

A monochromatic wave is propagating in the positive z direction. $\boldsymbol{\beta}_0 = \beta_0 \mathbf{e}_z$ and $\omega_0 = c\beta_0$ are its wave vector and (angular) frequency in vacuum, respectively.
c is the speed of light in vacuum. The medium is inhomogeneous, with a index of refraction $n(\mathbf{x})$

$$n(\mathbf{x}) = \begin{cases} n_c & \text{if } x^2 + y^2 > r^2 \\ n_a & \text{if } x^2 + y^2 \leq r^2 \end{cases} \tag{1.3}$$

Starting from Faraday-Lenz equation, taking the curl of both sides and using Ampère-Maxwell equation (with no free charges or currents since we are in a dielectric), the wave equation for the electric field is obtained.

$$\nabla^2 \mathbf{E}(\mathbf{x}, t) - \frac{n^2(\mathbf{x})}{c^2} \frac{\partial^2}{\partial t^2} \mathbf{E}(\mathbf{x}, t) = 0 \tag{1.4}$$

The full solution to this equation can be found [6] but we are only interested in an approximate one. Under the conditions of paraxial approximation, which is well satisfied by a single mode fiber, and of weak guidance (i.e. $\frac{n_a - n_c}{n_a} \ll 1$)[4], the scalar approximation can be used [5]. The x and y components of the electric field (or whatever two perpendicular linear polarizations one desires in the xy plane, owing to the axial symmetry of the system around z) decouple. These two indipendent modes of propagation are called LP_{01}. We write the field in the following way

$$E(\mathbf{x}, t) = \alpha_0 \mathcal{E}(\mathbf{x}) e^{i(\beta_0 n_c z - \omega_0 t)} \tag{1.5}$$

where α_0 is an arbitrary complex constant and $\mathcal{E}(\mathbf{x})$ is the time-independent envelope. After substituting the scalar field in in Eqn. (1.4) we get

$$\begin{aligned} &\Big(\frac{\partial^2}{\partial x^2} + \frac{\partial^2}{\partial y^2}\Big) E(\mathbf{x}, t) + \alpha_0 \frac{\partial^2 \mathcal{E}(\mathbf{x})}{\partial z^2} e^{i(\beta_0 n_c z - \omega_0 t)} + 2i\alpha_0 \beta_0 n_c \frac{\partial \mathcal{E}(\mathbf{x})}{\partial z} e^{i(\beta_0 n_c z - \omega_0 t)} \\ &- \alpha_0 \beta_0^2 n_c^2 \mathcal{E}(\mathbf{x}) e^{i(\beta_0 n_c z - \omega_0 t)} + \frac{\omega_0^2 n^2(\mathbf{x})}{c^2} \alpha_0 e^{i(\beta_0 n_c z - \omega_0 t)} \mathcal{E}(\mathbf{x}) = 0 \end{aligned} \tag{1.6}$$

and neglecting the second order partial derivative with respect to space in the paraxial approximation

$$\Big|\frac{\partial^2 \mathcal{E}}{\partial z^2}\Big| \ll \beta_0 \Big|\frac{\partial \mathcal{E}}{\partial z}\Big| \tag{1.7}$$

we obtain the following equation

$$i\hbar \frac{\partial}{\partial \tau} \mathcal{E}(x, y; \tau) = -\frac{\hbar^2}{2\hbar^2 \beta_0^2 n_s^2} \nabla_\perp^2 \mathcal{E}(x, y; \tau) + \frac{n_c^2 - n^2(\mathbf{x})}{2n_c^2} \mathcal{E}(x, y; \tau) \tag{1.8}$$

where $\tau = \hbar \beta_0 n_c z$ and $\nabla_\perp^2 = \frac{\partial^2}{\partial x^2} + \frac{\partial^2}{\partial y^2}$.
This is formally a Schrödinger equation; indeed it is called the optical Schrödinger equation, with "wave function" $\mathcal{E}$ for a fictitious particle of "mass" $\hbar^2 \beta_0^2 n_c^2$ evolving in "time" τ in a "potential"

$$V(\mathbf{x}) = \frac{n_c^2 - n^2(\mathbf{x})}{2n_c^2} \simeq \frac{n_c - n(\mathbf{x})}{n_c} \tag{1.9}$$

The "probability density" will be proportional to the square modulus of $\mathcal{E}$, itself proportional to the intensity of the field. We have exchanged time evolution with

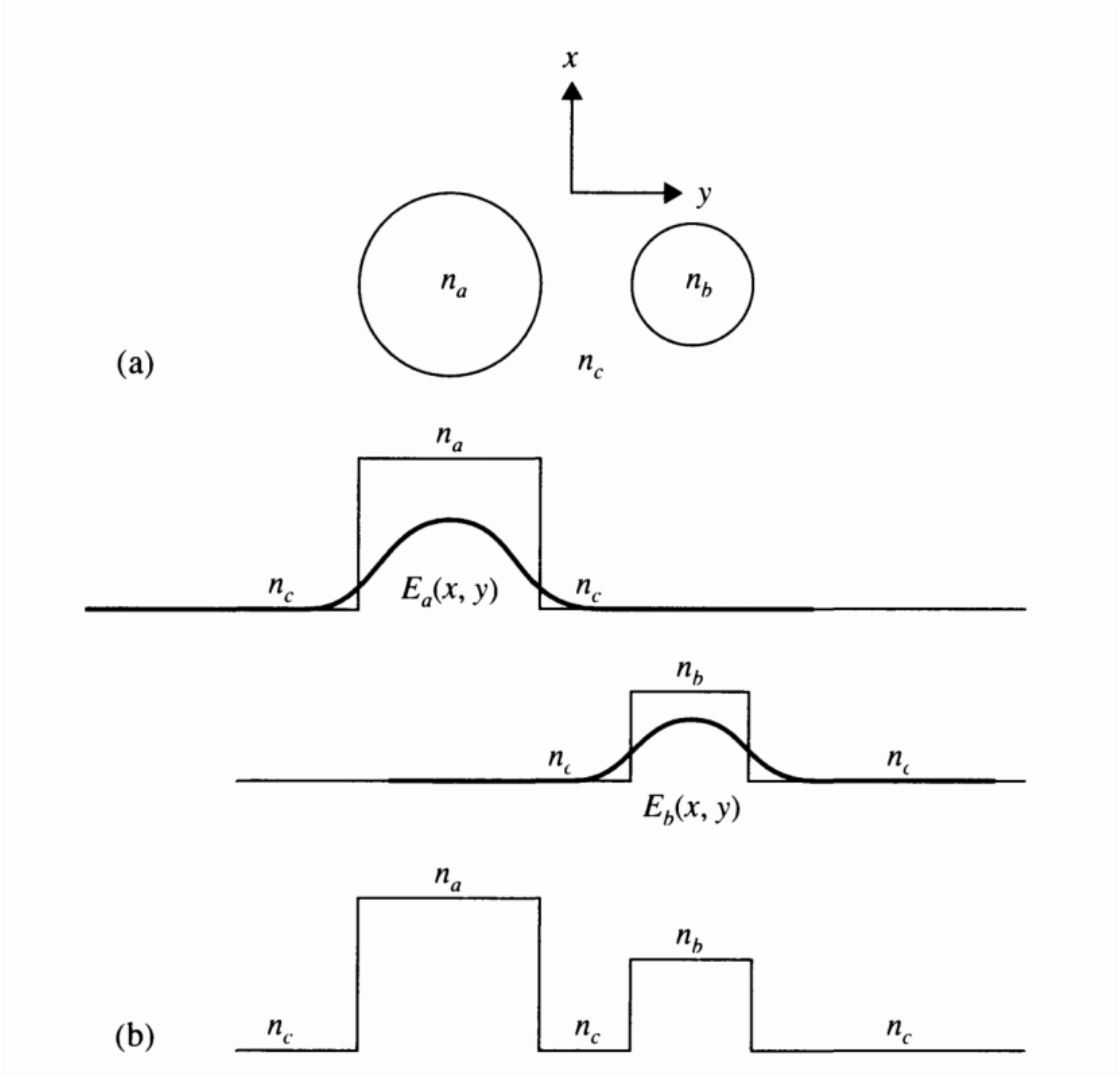

Figure 1.1: (a) Two parallel circular dielectric waveguides with axes along the z direction, perpendicular to the plane xy. (b) Profiles of the uncoupled guided modes and refractive indices. n_a and n_b are the core indices and n_c is the substrate (clad) index. [6].

space propagation along the fiber axis. As assumed, we have one guided mode, which is the equivalent to a bound state in a finite potential well with cylindrical symmetry. The exact shape of the field amplitude, as a function of x and y, can be calculated [6]. The important characteristics are that the amplitude of the field is axial symmetric, bell-shaped, maximum at the center and, outside the core of the fiber, it decays exponentially. Being a mode of the fiber, it does not change during the propagation, just like the lowest bound energy eigenstate of the quantum well, which is a stationary state in time.

The next step is to couple two parallel fibers by putting them close enough so that they can "feel" each other through the overlapping of the respective fields outside the core. This is called "evanescent coupling". The phenomenon is similar to the tunneling of an electron between two wells separated by a finite potential barrier. Referring to Figure 1.1, the fibers have refractive index n_a and n_b. The

substrate has refractive index n_c. The refractive index of the composite waveguide structure can be written as

$$n^2(x,y) = \begin{cases} n_a^2, & \text{core } a \quad (1.10) \\ n_b^2, & \text{core } b \quad (1.11) \\ n_c^2, & \text{elsewhere (substrate)} \quad (1.12) \end{cases}$$

In coupled-mode theory [6], a general wave propagation in the coupled-waveguide structure can be approximated, if the two waveguides are not too close to each other, by

$$\mathbf{E}(x,y,z,t) = A(z)\boldsymbol{\mathcal{E}}_a(x,y)e^{i(\beta_a z-\omega_0 t)} + B(z)\boldsymbol{\mathcal{E}}_b(x,y)e^{i(\beta_b z-\omega_0 t)} \tag{1.13}$$

when $\boldsymbol{\mathcal{E}}_a(x,y)e^{i(\beta_a z-\omega_0 t)}$ and $\boldsymbol{\mathcal{E}}_b(x,y)e^{i(\beta_b z-\omega_0 t)}$ are the only confined modes of propagation of the individual waveguides when they are far apart. β_a and β_b are the propagation constants in the two fibers. If the two waveguides do not interact, when an infinite distance is placed between them, $A(z)$ and $B(z)$ do not depend on z and each term on the right-hand side of Eqn. (1.13) satisfy the wave equation separately. To express this in a simple form, let's define the following quantities

$$\Delta n_a^2(x,y) = \begin{cases} n_a^2 - n_c^2, & \text{core } a \quad (1.14) \\ 0, & \text{elsewhere} \quad (1.15) \end{cases}$$

$$\Delta n_b^2(x,y) = \begin{cases} n_b^2 - n_c^2, & \text{core } b \quad (1.16) \\ 0, & \text{elsewhere} \quad (1.17) \end{cases}$$

Then we can write

$$n^2(x,y) = n_c^2 + \Delta n_a^2(x,y) + \Delta n_b^2(x,y) \tag{1.18}$$

We can thus say that

$$\Big(\nabla_\perp^2 + \frac{\omega_0^2}{c^2}[n_c^2 + \Delta n_\alpha^2(x,y)]\Big)\boldsymbol{\mathcal{E}}_\alpha(x,y) = \beta_\alpha^2\boldsymbol{\mathcal{E}}_\alpha(x,y) \tag{1.19}$$

with $\alpha = 1, 2$.
The field expressed in Eqn. (1.13) must satisfy the wave equation in the composite structure

$$\Big(\nabla_\perp^2 + \frac{\omega_0^2}{c^2}[n_c^2 + \Delta n_a^2(x,y) + \Delta n_b^2(x,y)]\Big)\mathbf{E} = 0 \tag{1.20}$$

Substituting Eqn. (1.13) into (1.20)

$$\begin{aligned}\Big(\nabla_\perp^2\mathbf{E} &+ \frac{\partial^2 A}{\partial z^2}\boldsymbol{\mathcal{E}}_a e^{i(\beta_a z-\omega_0 t)} + 2i\beta_a\frac{\partial A}{\partial z}\boldsymbol{\mathcal{E}}_a e^{i(\beta_a z-\omega_0 t)} - \beta_a^2 A\boldsymbol{\mathcal{E}}_a e^{i(\beta_a z-\omega_0 t)} \\ &+ \frac{\partial^2 B}{\partial z^2}\boldsymbol{\mathcal{E}}_b e^{i(\beta_b z-\omega_0 t)} + 2i\beta_b\frac{\partial B}{\partial z}\boldsymbol{\mathcal{E}}_b e^{i(\beta_b z-\omega_0 t)} - \beta_b^2 B\boldsymbol{\mathcal{E}}_b e^{i(\beta_b z-\omega_0 t)}\Big) + \frac{\omega_0^2}{c^2}n^2\mathbf{E} = 0\end{aligned} \tag{1.21}$$

Under the assumption of slow variation of the mode amplitudes $A(z)$ and $B(z)$ over z (paraxial approximation), we neglect the $2nd$ partial derivatives with respect to

z. Also, using Eqn. (1.19), we have

$$\begin{aligned}\nabla_\perp^2\mathbf{E}+\frac{\omega_0^2}{c^2}n^2\mathbf{E}=&\left(\beta_a^2-\frac{\omega_0^2}{c^2}(n_c^2+\Delta n_a^2)+\frac{\omega_0^2}{c^2}n^2\right)A\boldsymbol{\mathcal{E}}_a e^{i(\beta_a z-\omega_0 t)}\\&+\left(\beta_b^2-\frac{\omega_0^2}{c^2}(n_c^2+\Delta n_b^2)+\frac{\omega_0^2}{c^2}n^2\right)B\boldsymbol{\mathcal{E}}_b e^{i(\beta_b z-\omega_0 t)}\end{aligned}\tag{1.22}$$

Simplifying the refractive indices

$$\begin{aligned}\nabla_\perp^2\mathbf{E}+\frac{\omega_0^2}{c^2}n^2\mathbf{E}=&\left(\beta_a^2+\frac{\omega_0^2}{c^2}\Delta n_b^2\right)A\boldsymbol{\mathcal{E}}_a e^{i(\beta_a z-\omega_0 t)}\\&+\left(\beta_b^2+\frac{\omega_0^2}{c^2}\Delta n_a^2\right)B\boldsymbol{\mathcal{E}}_b e^{i(\beta_b z-\omega_0 t)}\end{aligned}\tag{1.23}$$

Substituting this result into Eqn. (1.21) (without the $2nd$ partial derivatives) we have

$$2i\beta_a\frac{\partial A}{\partial z}\boldsymbol{\mathcal{E}}_a e^{i\beta_a z}+\frac{\omega_0^2}{c^2}\Delta n_b^2 A\boldsymbol{\mathcal{E}}_a e^{i\beta_a z}+2i\beta_b\frac{\partial B}{\partial z}\boldsymbol{\mathcal{E}}_b e^{i\beta_b z}+\frac{\omega_0^2}{c^2}\Delta n_a^2 B\boldsymbol{\mathcal{E}}_b e^{i\beta_b z}=0\tag{1.24}$$

Taking the product of Eqn (1.24) with $\boldsymbol{\mathcal{E}}_a(x,y)^*$ and $\boldsymbol{\mathcal{E}}_b(x,y)^*$, respectively, and then integrating over the whole plane xy, with the assumption that the two fibers are not too close together, meaning

$$\iint\limits_{\mathbb{R}^2}\boldsymbol{\mathcal{E}}_a^*\cdot\boldsymbol{\mathcal{E}}_b\,dx\,dy\ll\iint\limits_{\mathbb{R}^2}\boldsymbol{\mathcal{E}}_a^*\cdot\boldsymbol{\mathcal{E}}_a\,dx\,dy\tag{1.25}$$

$$\iint\limits_{\mathbb{R}^2}\boldsymbol{\mathcal{E}}_a^*\cdot\boldsymbol{\mathcal{E}}_b\,dx\,dy\ll\iint\limits_{\mathbb{R}^2}\boldsymbol{\mathcal{E}}_b^*\cdot\boldsymbol{\mathcal{E}}_b\,dx\,dy\tag{1.26}$$

and using the normalization condition (since modes form a complete orthogonal set)

$$\frac{\beta_m}{2\omega_0\mu}\iint\limits_{\mathbb{R}^2}\boldsymbol{\mathcal{E}}_m\cdot\boldsymbol{\mathcal{E}}_n^*dx\,dy=\delta_{m,n}\tag{1.27}$$

where μ is the permeability of the medium, we finally arrive at the dynamic equations for the mode amplitudes $A(z)$ and $B(z)$

$$\begin{cases}\dfrac{dA}{dz}=i\kappa_{aa}A+i\kappa_{ab}Be^{i(\beta_b-\beta_a)z} & (1.28)\\[2ex] \dfrac{dB}{dz}=i\kappa_{ba}Ae^{i(\beta_a-\beta_b)z}+i\kappa_{bb}B & (1.29)\end{cases}$$

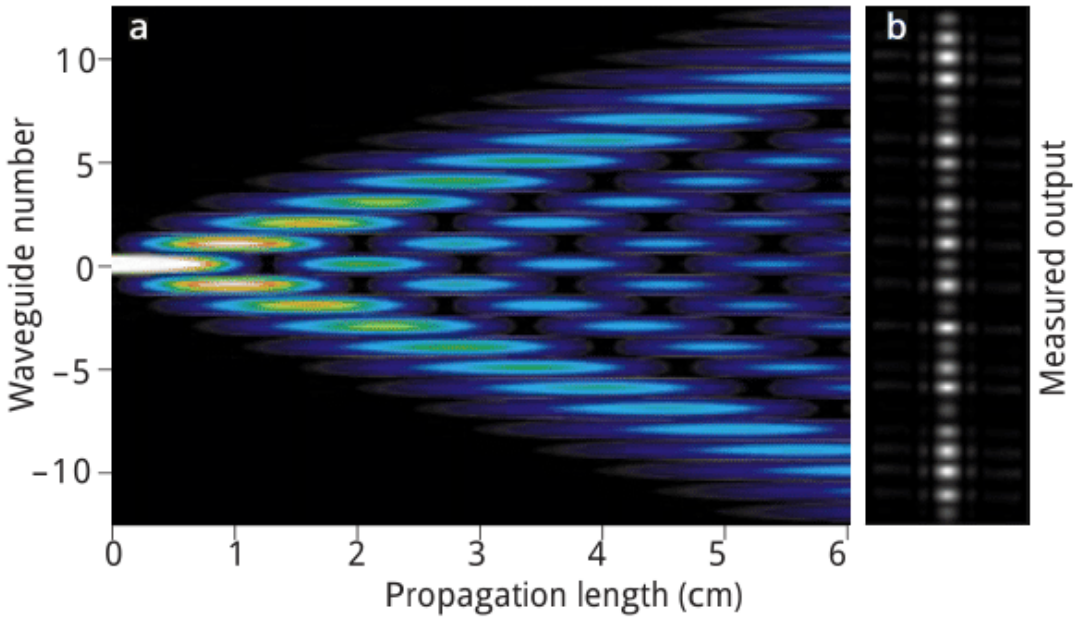

Figure 1.2: **a**) A numerical simulation of a narrow input beam that excites a single site of a periodically poled lithium niobate waveguide array with a spacing between waveguides of 15 μm and a wavelength of 1.56 μm. **b**) Experimental measurement of the intensity distribution at the output facet of a lithium niobate waveguide array at $1,56$ μm. [20].

where

$$\kappa_{aa} = \frac{\omega_0}{4}\varepsilon_0 \iint_{\mathbb{R}^2} \boldsymbol{\mathcal{E}}_a^* \cdot \Delta n_b^2 \boldsymbol{\mathcal{E}}_a \, dx \, dy \tag{1.30}$$

$$\kappa_{bb} = \frac{\omega_0}{4}\varepsilon_0 \iint_{\mathbb{R}^2} \boldsymbol{\mathcal{E}}_b^* \cdot \Delta n_a^2 \boldsymbol{\mathcal{E}}_b \, dx \, dy \tag{1.31}$$

$$\kappa_{ab} = \frac{\omega_0}{4}\varepsilon_0 \iint_{\mathbb{R}^2} \boldsymbol{\mathcal{E}}_a^* \cdot \Delta n_a^2 \boldsymbol{\mathcal{E}}_b \, dx \, dy \tag{1.32}$$

$$\kappa_{ba} = \frac{\omega_0}{4}\varepsilon_0 \iint_{\mathbb{R}^2} \boldsymbol{\mathcal{E}}_b^* \cdot \Delta n_b^2 \boldsymbol{\mathcal{E}}_a \, dx \, dy \tag{1.33}$$

and where ε_0 is the permittivity of free space. The terms κ_{aa} and κ_{bb} result from perturbations in one waveguide due to the presence of the other waveguide and are generally small with respect to the propagation constants β_a and β_b, respectively. We will assume them to be negligible throughout this discussion. κ_{ab} and κ_{ba} are the exchange couplings between the two waveguides. It can be shown, imposing conservation of energy, that $\kappa_{ab} = \kappa_{ba}^*$. This coupling phenomenon between modes is similar to the electron motion in a two-atom molecule. Putting together a large number of weakly coupled parallel waveguides, the optical analog to single-particle quantum transport in a quantum wire is realized. In this sense, coupled-mode theory is like tight-binding approximation in solid state physics. In Figure 1.2 it is

shown a visualization of what happens when light is launched in a waveguide array; in Figure 1.2(a) a numerical simulation of the distribution of light is calculated while, in Figure 1.2(b) an actual measurement of light intensity at the output facet of an actual structure is presented [20].
Reaching the continuum is now easy. Just extend the array of parallel waveguides to infinity.
To simulate the discrete states embedded in the continuum, waveguides are side-couple to the array. It is important to note that the conditions under which coupled-mode theory is valid, are compatible with the derivation of the optical Schrödinger equation, so they can be used together.

Chapter 2

Fano resonance and bound states in the continuum

The optical structure, in which Fano resonances are present, is shown in Figure 2.1(a). In the analysis, a new important feature will emerge, bound states in the continuum (BIC).
An infinite array of evanescently coupled optical waveguides is side-coupled to N waveguides $|1\rangle$, $|2\rangle$, ..., $|\alpha\rangle$, ..., $|N\rangle$. Coupled-mode theory is assumed to be valid, so each waveguide is weakly coupled to the next one. κ_α is the coupling rate between the side waveguide $|\alpha\rangle$ and the waveguide of index n_α in the array ($\alpha = 1, 2, ..., N$), whereas the coupling rate between adjacent waveguides in the linear array is κ. The zero index in the array can be chosen arbitrarily; for example, looking at Figure 2.1(a) with $N = 4$, and choosing $n_2 = 0$, one has $n_1 = -2$, $n_{\alpha=3} = 3$ and $n_4 = 6$.

Indicating by $b_n(z)$ the field amplitude of light waves trapped in the waveguide n of the infinite linear array, and by $\tilde{c}_\alpha(z)$ the field amplitude of light waves trapped in the side waveguide $|\alpha\rangle$, the evolution of modal amplitudes along the spatial propagation distance z, using Eqns. (1.28) and (1.29), is governed by the following set of coupled-mode equations:

$$\begin{cases} \dfrac{db_n}{dz} = i\kappa(b_{n+1} + b_{n-1}) + i\displaystyle\sum_{\alpha=1}^{N} \kappa_\alpha \tilde{c}_\alpha e^{i(\beta_\alpha - \beta)z}\delta_{n,n_\alpha} & (n \in \mathbb{Z}) \qquad (2.1) \\ \dfrac{d\tilde{c}_\alpha}{dz} = i\kappa_\alpha b_{n_\alpha} e^{i(\beta - \beta_\alpha)z} & (\alpha = 1, 2, ..., N) \qquad (2.2) \end{cases}$$

where $\mathbb{Z}$ is the set of integer numbers. Define

$$c_\alpha(z) \equiv \tilde{c}_\alpha(z) e^{-i\omega_\alpha z} \qquad (2.3)$$

where $\omega_\alpha = \beta - \beta_\alpha$ is the propagation constant mismatch between the side waveguide $|\alpha\rangle$ and the waveguide in the array. We then obtain

$$\begin{cases} i\dfrac{db_n}{dz} = -\kappa(b_{n+1} + b_{n-1}) - \displaystyle\sum_{\alpha=1}^{N} \kappa_\alpha c_\alpha \delta_{n,n_\alpha} & (n \in \mathbb{Z}) \qquad (2.4) \\ i\dfrac{dc_\alpha}{dz} = -\kappa_\alpha b_{n_\alpha} + \omega_\alpha c_\alpha & (\alpha = 1, 2, ..., N) \qquad (2.5) \end{cases}$$

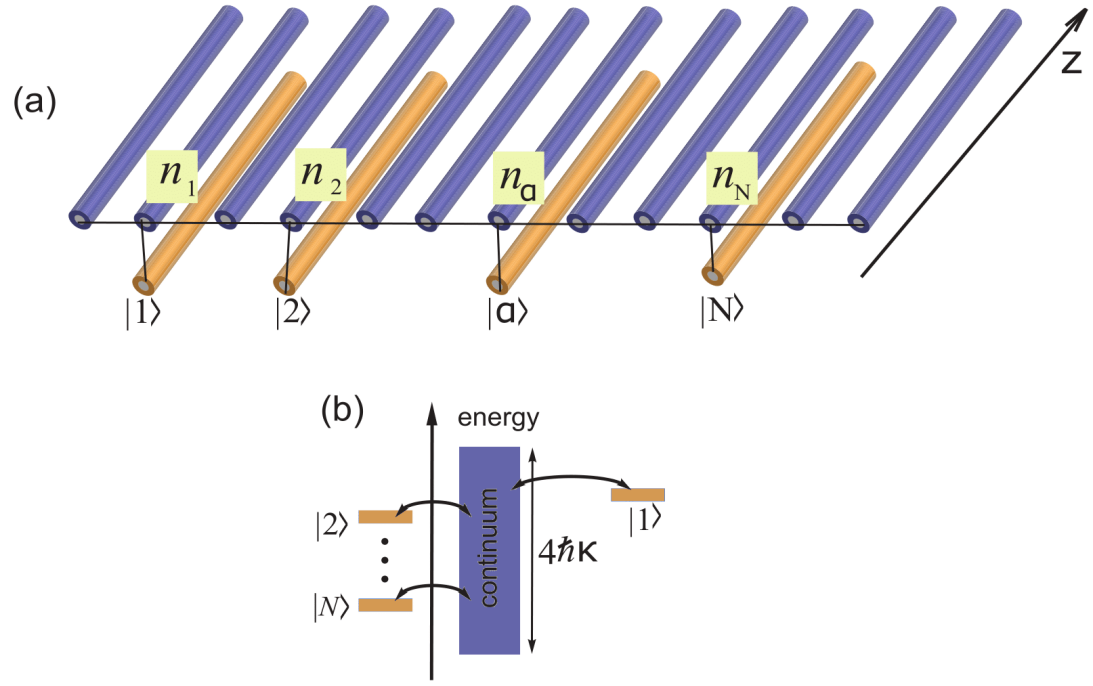

Figure 2.1: (a) Optical structure made up of N waveguides. $|1\rangle$, $|2\rangle$, ..., $|N\rangle$, side-coupled to an infinite array of waveguides. (b) The quantum analogue of the waveguide structure in (a), with N discrete states coupled to continuum states.

Typically, light is launched into one of the side waveguides, which is equivalent to populating one of the corresponding discrete levels; see Figure 2.1(b). Light decays though evanescent coupling into a featureless (only one waveguide side-coupled to the array) or structured (more than one waveguide side coupled to the array) continuum, the same as population on a discrete level decays into the continuum. To make the analogy between quantum mechanics and optics even more clear, we perform a change of basis in Eqn. (2.4) and (2.5), going from a Wannier basis to a Bloch basis. We introduce the amplitude $c(k, z)$ which is a function of the Bloch wave number k, defined in the first Brillouin zone, $-\pi \leq k < \pi$, where we have assumed unit distance between the waveguides in the array:

$$c(k, z) = -\frac{1}{\sqrt{2\pi}} \sum_{n \in \mathbb{Z}} b_n(z) e^{ikn} \tag{2.6}$$

and the corresponding inversion relation

$$b_n(z) = -\frac{1}{\sqrt{2\pi}} \int_{-\pi}^{\pi} dk\, c(k, z) e^{-ikn} \tag{2.7}$$

We are just borrowing nomenclature and results from solid state physics, since we are dealing with a periodic structure and, mathematically, everything is formally the same. Since this array is infinite, k is a continuum variable.

Multiplying Eqn. (2.4) by e^{ikn} and summing over n

$$\begin{aligned}
&\sum_{n\in\mathbb{Z}} i\frac{db_n}{dz}e^{ikn} = -\kappa\sum_{n\in\mathbb{Z}}(b_{n+1}e^{ikn}+b_{n-1}e^{ikn}) - \sum_{n\in\mathbb{Z}}\sum_{\alpha=1}^{N}\kappa_\alpha c_\alpha e^{ikn}\delta_{n,n_\alpha}\\
&i\frac{d}{dz}\sum_{n\in\mathbb{Z}} b_n e^{ikn} = -\kappa e^{-ik}\sum_{n\in\mathbb{Z}} b_{n+1}e^{ik(n+1)} - \kappa e^{ik}\sum_{n\in\mathbb{Z}} b_{n-1}e^{ik(n-1)} - \sum_{\alpha=1}^{N}\kappa_\alpha c_\alpha e^{ikn_\alpha}\\
&i\frac{d}{dz}\sum_{n\in\mathbb{Z}} b_n e^{ikn} = -\kappa(e^{-ik}+e^{ik})\sum_{n\in\mathbb{Z}} b_n e^{ikn} - \sum_{\alpha=1}^{N}\kappa_\alpha c_\alpha e^{ikn_\alpha}\\
&i\frac{d}{dz}\sum_{n\in\mathbb{Z}} b_n e^{ikn} = -2\kappa\cos k\sum_{n\in\mathbb{Z}} b_n e^{ikn} - \sum_{\alpha=1}^{N}\kappa_\alpha c_\alpha e^{ikn_\alpha}\\
&i\frac{d}{dz}c(k,z) = -2\kappa\cos k(c(k,z)) + \frac{1}{\sqrt{2\pi}}\sum_{\alpha=1}^{N}\kappa_\alpha c_\alpha e^{ikn_\alpha}
\end{aligned} \tag{2.8}$$

and using Eqn. (2.7) in Eqn. (2.5)

$$i\frac{dc_\alpha}{dz} = \omega_\alpha c_\alpha + \frac{\kappa_\alpha}{\sqrt{2\pi}}\int_{-\pi}^{\pi} dk\, c(k,z)e^{-ikn_\alpha} \tag{2.9}$$

we obtain the system

$$\begin{cases}
i\dfrac{dc}{dz} = \omega(k)c(k,z) + \displaystyle\sum_{\alpha=1}^{N} g_\alpha(k)c_\alpha(z) & (2.10)\\
i\dfrac{dc_\alpha}{dz} = \omega_\alpha c_\alpha(z) + \displaystyle\int_{-\pi}^{\pi} dk\, g_\alpha^*(k)c(k,z) \qquad (\alpha = 1,\, 2,\, ...,\, N) & (2.11)
\end{cases}$$

where

$$\omega(k) = -2\kappa\cos k \quad , \quad g_\alpha(k) = \frac{\kappa_\alpha}{\sqrt{2\pi}}e^{ikn_\alpha} \tag{2.12}$$

If we exchange the spatial coordinate z with time t, Eqns. (2.10) and (2.11) describe the quantum evolution in time of a system made up of N discrete levels $|1\rangle$, $|2\rangle$, ..., $|N\rangle$ of energy $\hbar\omega_1$, $\hbar\omega_2$, ..., $\hbar\omega_N$, coupled to a continuum (a band) of states $|k\rangle$ with energy $\hbar\omega(k)$, ranging from $-2\hbar\kappa$ to $2\hbar\kappa$. The model describing such a system is known as Fano-Anderson model, having the following Hamiltonian

$$\hat{H} = \hbar\sum_{\alpha=1}^{N}\omega_\alpha\,|\alpha\rangle\langle\alpha| + \hbar\int dk\,\omega(k)\,|k\rangle\langle k| + \hbar\sum_{\alpha=1}^{N}\int dk\,(g_\alpha^*(k)\,|\alpha\rangle\langle k| + g_\alpha(k)\,|k\rangle\langle\alpha|) \tag{2.13}$$

where $g_\alpha(k)$ is the coupling amplitude between states $|\alpha\rangle$ and $|k\rangle$ and the integrals are over the appropriate range. If we expand a general solution $|\psi\rangle$ in the complete set of energy eigenstates

$$|\psi\rangle = \sum_{\alpha=1}^{N} c_\alpha(t)\,|\alpha\rangle + \int dk\, c(k,t)\,|k\rangle \tag{2.14}$$

and substitute it inside the Schrödinger equation, assuming orthonormality, such that $\langle\alpha|\beta\rangle = \delta_{\alpha,\beta}$, $\langle\alpha|k\rangle = 0$ and $\langle k|k'\rangle = \delta(k-k')$, we get

$$i\hbar\frac{\partial}{\partial t}|\psi\rangle = i\hbar\sum_{\alpha=1}^{N}\frac{\partial c_\alpha}{\partial t}|\alpha\rangle + i\hbar\int_{-\pi}^{\pi}dk\,\frac{\partial c(k,t)}{\partial t}|k\rangle = \hat{H}|\psi\rangle \tag{2.15}$$

$$\begin{aligned}\hat{H}|\psi\rangle = \hbar\sum_{\alpha=1}^{N}\omega_\alpha c_\alpha|\alpha\rangle + \hbar\sum_{\alpha=1}^{N}\int dk\,g_\alpha(k)c_\alpha|k\rangle + \hbar\int dk\,\omega(k)c(k,t)|k\rangle \\ + \hbar\sum_{\alpha=1}^{N}\int dk\,g_\alpha^*(k)c(k,t)|\alpha\rangle\end{aligned} \tag{2.16}$$

Multiplying on the left Eqn. (2.15) by $\langle k'|$ and by $\langle\beta|$ respectively and renaming dummy indices $\beta \to \alpha$ and $k' \to k$, we obtain Eqns. (2.10) and (2.11), in time t instead of space z. In our optical analogue of the quantum mechanical decay problem we have replaced time evolution of quantum states with spatial propagation along the axis z. Fractional power in waveguide $|\alpha\rangle$, proportional to $|c_\alpha(z)|^2$, plays the role of population for level $|\alpha\rangle$, or the probability that, in a measurement, the system is found in level $|\alpha\rangle$.

An analytical solution of Eqns. (2.10) and (2.11) is generally not possible. An approximate solution can be found in a simple, but relevant case, which shows Fano resonance and BIC. The assumption is weak coupling between the discrete states and the continuum, or, in our optical model, the coupling between waveguides in the array is stronger than that between the array and the side-coupled waveguides, i.e. $\kappa \gg \kappa_\alpha$. Considering the Eqns. (2.10) and (2.11), we want to eliminate the amplitudes $c(k,z)$. Start by assuming, without loss of generality, $c(k,z) = f(k,z)e^{-i\omega(k)z}$ and $c_\alpha(z) = f_\alpha(z)e^{-i\omega_\alpha z}$ and substitute into Eqn. (2.10)

$$i\Big(\frac{\partial f}{\partial z}e^{-i\omega z} - if\omega e^{-i\omega z}\Big) = \omega f e^{-i\omega z} + \sum_{\alpha=1}^{N} g_\alpha f_\alpha e^{-i\omega_\alpha z}$$

$$\frac{\partial f}{\partial z} = -i\sum_{\alpha=1}^{N} g_\alpha f_\alpha e^{i(\omega-\omega_\alpha)z}$$

Integrating from the initial point at $z = 0$ up to z, assuming $f(k,0) = 0$, meaning no light is injected in the array of waveguides at $z = 0$, we get

$$f(k,z) = -i\int_0^z dz' \sum_{\alpha=1}^{N} g_\alpha f_\alpha e^{i(\omega-\omega_\alpha)z}$$

Going back to the field amplitudes

$$c(k,z) = -i\int_0^z dz' \sum_{\beta=1}^{N} g_\beta c_\beta e^{i\omega(z'-z)}$$

Substituting this result into Eqn. (2.11), we obtain a system of integrodifferential equations for the field amplitudes $c_\alpha(z)$ in the side waveguides

$$\frac{dc_\alpha}{dz} = -i\omega_\alpha c_\alpha(z) - \sum_{\beta=1}^{N}\int_0^z dz'\,\Phi_{\alpha,\beta}(z-z')c_\beta(z') \tag{2.17}$$

where

$$\Phi_{\alpha,\beta}(z-z') \equiv \int_{-\pi}^{\pi} dk\, g_\alpha^*(k) g_\beta(k) e^{-i\omega(k)(z-z')} \tag{2.18}$$

are called the "memory functions", which can be calculated for the specific functions in Eqns. (2.12)

$$\Phi_{\alpha,\beta}(z-z') = i^{n_\alpha - n_\beta} \kappa_\alpha \kappa_\beta J_{n_\alpha - n_\beta}(2\kappa(z-z')) \tag{2.19}$$

where J_n is the Bessel function of order n. For $n \in \mathbb{Z}$, with real x, $J_n(x)$ is finite at the origin ($x = 0$) and looks roughly like oscillating sine or cosine functions that decay proportionally to $1/\sqrt{x}$, although their roots are not generally periodic, except asymptotically for large x; also, $J_{-n}(x) = (-1)^n J_n(x)$. We now want to calculate an approximate expression for the integral in Eqn. (2.17). An analytical solution to this equation is not easy to find because the process it describes is a non-Markovian one, meaning that it depends on the solution itself at all previous positions. Having assumed that $\kappa_\alpha \ll \kappa$, for ω_α in the continuum and far from band edges $\pm 2\kappa$, setting $c_\alpha(z) = q_\alpha(z) e^{-i\omega_\alpha z}$, we have that $q_\alpha(x)$ varies slowly over the "period" $\sim 1/\kappa$ of the memory function (a Bessel function).

$$\int_0^z dz'\, \Phi_{\alpha,\beta}(z-z') c_\beta(z') = \int_0^z dz'\, \Phi_{\alpha,\beta}(z-z') q_\beta(z') e^{-i\omega_\beta z'} \tag{2.20}$$

Under these assumptions, we make the Markov approximation, in which $q(z')$ is replaced by its value at the upper limit of the integral and so it can be taken out

$$\int_0^z dz'\, \Phi_{\alpha,\beta}(z-z') q_\beta(z') e^{-i\omega_\beta z'} = q_\beta(z) \int_0^z dz'\, \Phi_{\alpha,\beta}(z-z') e^{-i\omega_\beta z'} \tag{2.21}$$

With the change of variable $z - z' = \tau$

$$\begin{aligned} \int_0^z dz'\, \Phi_{\alpha,\beta}(z-z') e^{-i\omega_\beta z'} &= \int_0^z d\tau\, \Phi_{\alpha,\beta}(\tau) e^{-i\omega_\beta z} e^{i\omega_\beta \tau} \\ &= e^{-i\omega_\beta z} \int_0^z d\tau\, \Phi_{\alpha,\beta}(\tau) e^{i\omega_\beta \tau} \end{aligned} \tag{2.22}$$

We finally have an approximate expression for Eqn. (2.17)

$$\frac{dc_\alpha}{dz} \simeq -i\omega_\alpha c_\alpha - \sum_{\beta=1}^{N} \Delta_{\alpha,\beta} c_\beta \tag{2.23}$$

where

$$\begin{aligned} \Delta_{\alpha,\beta} &= \int_0^\infty d\tau\, \Phi_{\alpha,\beta}(\tau) e^{i\omega_\beta \tau} = \\ &= \kappa_\alpha \kappa_\beta i^{|n_\alpha - n_\beta|} \frac{\left(\sqrt{4\kappa^2 - \omega_\beta^2} + i\omega_\beta\right)^{|n_\alpha - n_\beta|}}{(2\kappa)^{|n_\alpha - n_\beta|} \sqrt{4\kappa^2 - \omega_\beta^2}} \end{aligned} \tag{2.24}$$

We begin the analysis of the optical structure when $N = 1$, with one waveguide side-coupled to the linear array. Light is launched into the side waveguide and

decays exponentially into the array. Nothing really interesting is happening. The governing equation is

$$\frac{dc_1}{dz} \simeq -(\Delta_{11} + i\omega_1)c_1 \tag{2.25}$$

where

$$\Delta_{11} = \frac{\kappa_1^2}{\sqrt{4\kappa^2 - \omega_1^2}} \tag{2.26}$$

The initial condition, at $z = 0$, is $c_1(0) = 1$. The solution is simply $c_1(z) = e^{-(\Delta_{11}+i\omega_1)z}$. Next we set $N = 2$, two side-coupled waveguides $|1\rangle$ and $|2\rangle$. Here we begin to see Fano resonance and BIC. The system evolves according to the following coupled equations

$$\begin{cases} \dfrac{dc_1}{dz} \simeq -(\Delta_{11} + i\omega_1)c_1 - \Delta_{12}c_1 & (2.27) \\ \dfrac{dc_2}{dz} \simeq -\Delta_{21}c_1 - (\Delta_{22} + i\omega_2)c_2 & (2.28) \end{cases}$$

Setting $n_1 = 0$ and $n_2 = n_0 > 0$, we have

$$\Delta_{11} = \frac{\kappa_1^2}{\sqrt{4\kappa^2 - \omega_1^2}} \tag{2.29}$$

$$\Delta_{22} = \frac{\kappa_2^2}{\sqrt{4\kappa^2 - \omega_2^2}} \tag{2.30}$$

$$\Delta_{12} = i^{n_0}\kappa_1\kappa_2 \frac{\left(\sqrt{4\kappa^2 - \omega_2^2} + i\omega_2\right)^{n_0}}{(2\kappa)^{n_0}\sqrt{4\kappa^2 - \omega_2^2}} \tag{2.31}$$

$$\Delta_{21} = i^{n_0}\kappa_1\kappa_2 \frac{\left(\sqrt{4\kappa^2 - \omega_1^2} + i\omega_1\right)^{n_0}}{(2\kappa)^{n_0}\sqrt{4\kappa^2 - \omega_1^2}} \tag{2.32}$$

The system of Eqns. (2.27) and (2.28) is solved, given initial conditions on the amplitudes, through the standard method of finding the eigenvalues and the corresponding eigenmodes. Population trapping or, equivalently, light in a side-coupled waveguide not decaying into the array, is linked to the vanishing of the real part of the corresponding eigenvalue. Physically, this derives from a destructive interference effect between different decay channels (tunneling paths) of light in waveguides into the array.

For our purposes, an interesting case arises when the coupling κ_1 of waveguide $|1\rangle$ to the linear array is much weaker than the other coupling κ_2 of waveguide $|2\rangle$. What we are modeling is the decay of a discrete level in a structured continuum, which is strongly coupled to the discrete level $|2\rangle$. The system of Eqns. (2.27) and (2.28), in the limit of $\kappa_1 \ll \kappa_2$, can be solved for the modal amplitude $c_1(z)$ (following a similar procedure in [15]). Define

$$c_1(z) \equiv s_1(z)e^{-i\omega_1 z}, \qquad c_2(z) \equiv s_2(z)e^{-i\omega_1 z} \tag{2.33}$$

and substitute it in Eqn. (2.28)

$$\frac{ds_2}{dz} = -\Delta_{21}s_1 - [\Delta_{22} + i(\omega_2 - \omega_1)]s_2 \tag{2.34}$$

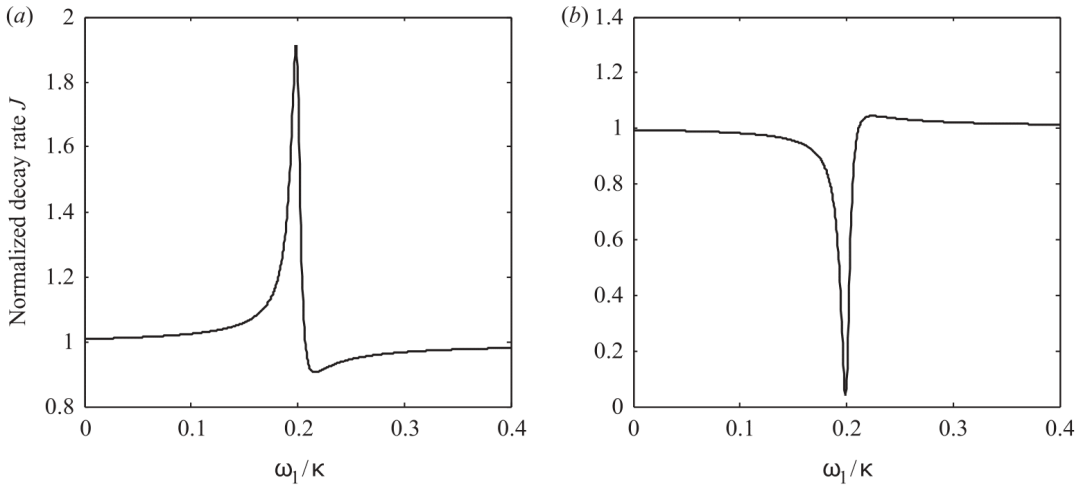

Figure 2.2: Fano resonance for $N = 2$ side waveguides. Normalized decay rate J of light in waveguide $|1\rangle$, weakly coupled to the array in the presence of a strongly coupled waveguide $|2\rangle$, is plotted versus normalized propagation constant mismatch ω_1/κ. Decay rate is normalized to the one in the absence of waveguide $|2\rangle$. Parameter values are: $\kappa_1/\kappa = 0.04$, $\kappa_2/\kappa = 0.1$, $\omega_2/\kappa = 0.2$ for (a) $n_0 = 3$ and for (b) $n_0 = 4$. The lineshape, around $\omega_1 = \omega_2$, is asymmetric, a typical sign of a Fano resonance.

since $\kappa_1 \ll \kappa_2$ implies $\Delta_{12} \ll \Delta_{22}$, and $s_2(0) = 0$, since light is launched only in waveguide $|1\rangle$, we can neglect the derivative of $s_2(z)$. Thus we have

$$s_2(z) \simeq -\frac{\Delta_{21}}{\Delta_{22} + i(\omega_2 - \omega_1)} s_1(z) \tag{2.35}$$

which means

$$c_2(z) \simeq -\frac{\Delta_{21}}{\Delta_{22} + i(\omega_2 - \omega_1)} c_1(z) \tag{2.36}$$

Using this result into Eqn. (2.27) we find

$$\frac{dc_1}{dz} \simeq \Big[-(\Delta_{11} + i\omega_1) + \frac{\Delta_{12}\Delta_{21}}{\Delta_{22} + i(\omega_2 - \omega_1)} \Big] c_1 \tag{2.37}$$

which, for $\kappa_2 = 0$ reduces to the case of a single waveguide $|1\rangle$ side-coupled to a featureless continuum. The functional dependence of the decay rate R (the negative real part in the square brackets of Eqn. (2.37)) of the light in waveguide $|1\rangle$ versus ω_1, normalized to its value Δ_{11} in the absence of waveguide $|2\rangle$ is

$$J \equiv \frac{R}{\Delta_{11}} = 1 - \mathrm{Re}\left\{ \frac{\Delta_{12}\Delta_{21}}{\Delta_{11}[\Delta_{22} + i(\omega_2 - \omega_1)]} \right\} \tag{2.38}$$

Typical behaviors of $J(\omega_1)$ are plotted in Figure 2.2. Notice the asymmetric shape. This is a Fano resonance. Around $\omega_1 = \omega_2$, with odd n_0, a strong peak is observed (Figure 2.2(a)), thus increasing the decay rate, while, with n_0 even, a strong dip appears (Figure 2.2(b)), decreasing the decay rate. In particular, at

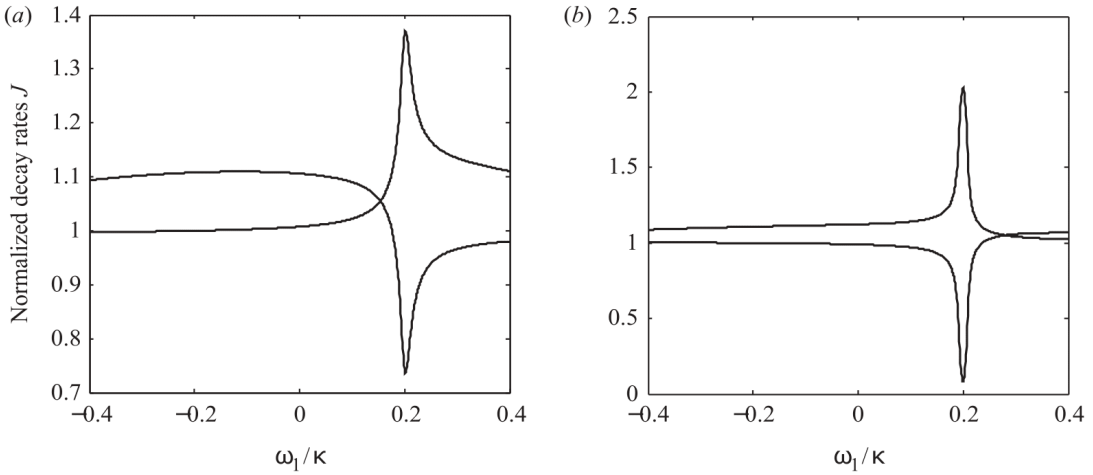

Figure 2.3: Fano resonance for $N = 2$ side waveguides. Normalized decay rates $J_{1,2} = -\,\mathrm{Re}(\lambda_{1,2})/\Delta_{11}$ versus normalized propagation constant mismatch ω_1/κ for parameter values $\kappa_1/\kappa = 0.095$, $\kappa_2/\kappa = 0.1$, $\omega_2/\kappa = 0.2$ and for (a) $n_0 = 3$, (b) $n_0 = 4$. [7].

$\omega_1 = \omega_2$ for $\omega_2 = 0$, J vanishes, leading to a complete suppression of the decay. Light is trapped in waveguide $|1\rangle$, which is the analogous of population trapping. This is a BIC. The position of waveguide $|2\rangle$, with respect to waveguide $|1\rangle$, can enhance or suppress, even completely, light decay in waveguide $|1\rangle$. A full solution of the system of Eqns. (2.27) and (2.28) can be calculated [7], without the restriction of strong coupling of waveguide $|2\rangle$ to the array. With the initial condition of $c_1(0) = 1$ and $c_2(0) = 0$ we get the following bi-exponential solutions:

$$c_1(z) = \frac{\Delta_{11} + \lambda_1 + i\omega_1}{\lambda_1 - \lambda_2} e^{\lambda_2 z} - \frac{\Delta_{11} + \lambda_2 + i\omega_1}{\lambda_1 - \lambda_2} e^{\lambda_1 z} \tag{2.39}$$

$$c_2(z) = \frac{(\Delta_{11} + \lambda_1 + i\omega_1)(\Delta_{11} + \lambda_2 + i\omega_1)}{\Delta_{12}(\lambda_1 - \lambda_2)} (e^{\lambda_1 z} - e^{\lambda_2 z}) \tag{2.40}$$

where λ_1 and λ_2 are the roots of the characteristic polynomial associated to the matrix of the coefficients of the system

$$\lambda^2 + (\Delta_{11} + \Delta_{22} + i\omega_1 + i\omega_2)\lambda - \Delta_{12}\Delta_{21} \tag{2.41}$$

$$+ (\Delta_{11} + i\omega_1)(\Delta_{22} + i\omega_2) = 0 \tag{2.42}$$

The power leakage into the continuum is $I(z) = 1 - |c_1(z)|^2 - |c_2(z)|^2$.
Again, asymmetric peaks and different behaviors, for n_0 odd or even, are observed; in Figure 2.3, normalized decay rate $J_{1,2} = -\,\mathrm{Re}(\lambda_{1,2})/\Delta_{11}$ is plotted versus ω_1. The asymptotic behavior is basically determined by the "slowest" decaying exponential. However, strong deviations from a single exponential decay law occur when κ_1 becomes comparable to κ_2.
Population trapping is achieved when the real part of either λ_1 or λ_2 vanishes. When $\omega_1 = \omega_2 = 0$, it is immediate to show that one root vanishes for any even

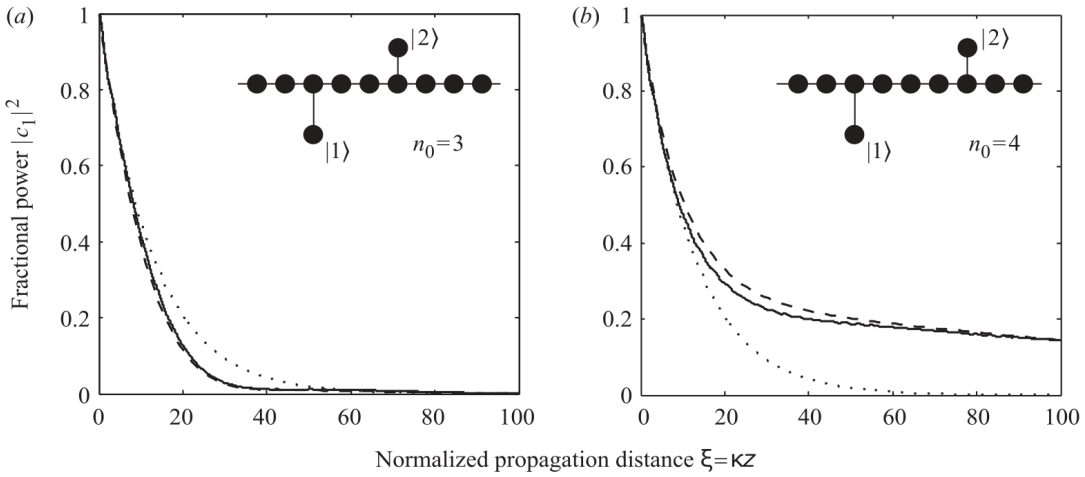

Figure 2.4: Light power $|c_1|^2$ in waveguide $|1\rangle$ versus normalized distance $\xi = \kappa z$, with a second waveguide $|2\rangle$ placed at (a) $n_0 = 3$ and (b) $n_0 = 4$ sites away from waveguide $|1\rangle$, as shown in the insets. Parameters values are: $\kappa_1/\kappa = 0.28$, $\kappa_2/\kappa = 0.3$ and $\omega_1/\kappa = \omega_2/\kappa = 0.2$. Solid lines correspond to numerically computed results. Dashed curves obtained from Eqn. (2.39). Dotted curves represent the decay one would observe in the absence of waveguide $|2\rangle$, i.e. $\kappa_2 = 0$. Note that the presence of waveguide $|2\rangle$ leads to an acceleration of the decay in (a) and a deceleration of the decay in (b). [7].

value of n_0. In this case we have

$$c_1(z) = \frac{1}{1+(\kappa_2/\kappa_1)^2}\exp\left[-\frac{(\kappa_1^2+\kappa_2^2)z}{2\kappa}\right] + \frac{1}{1+(\kappa_1/\kappa_2)^2} \tag{2.43}$$

$$c_2(z) = -\frac{\kappa_1\kappa_2}{i^{n_0}(\kappa_1^2+\kappa_2^2)}\left\{1-\exp\left[-\frac{(\kappa_1^2+\kappa_2^2)z}{2\kappa}\right]\right\} \tag{2.44}$$

After the transients, the fractional power in waveguides $|1\rangle$ and $|2\rangle$ is

$$|c_1(\infty)|^2 = \left[\frac{1}{1+(\kappa_1/\kappa_2)^2}\right]^2 \tag{2.45}$$

$$|c_2(\infty)|^2 = \left(\frac{\kappa_1}{\kappa_2}\right)^2\left[\frac{1}{1+(\kappa_1/\kappa_2)^2}\right]^2 \tag{2.46}$$

and the power leaked into the continuum $I(\infty) = \kappa_1^2/(\kappa_1^2+\kappa_2^2)$. Beyond the Markovian approximation, only numerical analysis is available. Such results are shown in Figure 2.4, where the fractional power in waveguide $|1\rangle$ is plotted in solid line versus the (normalized) distance z along the guide, at resonance $\omega_1 = \omega_2$. Dashed line represents the results with Markovian approximation. Also shown, in dotted line, the decay law in the absence of the second side-coupled waveguide $|2\rangle$. Notice the expected behavior with odd n_0 (Figure 2.4(a)), where we see an increased acceleration of the decay; on the contrary, with even n_0 (Figure 2.4(b)) we see a deceleration of the decay. The case of population trapping, for $\omega_1 = \omega_2 = 0$ and n_0 even is shown in Figure 2.5 (with the same meaning as before for solid and dashed lines).

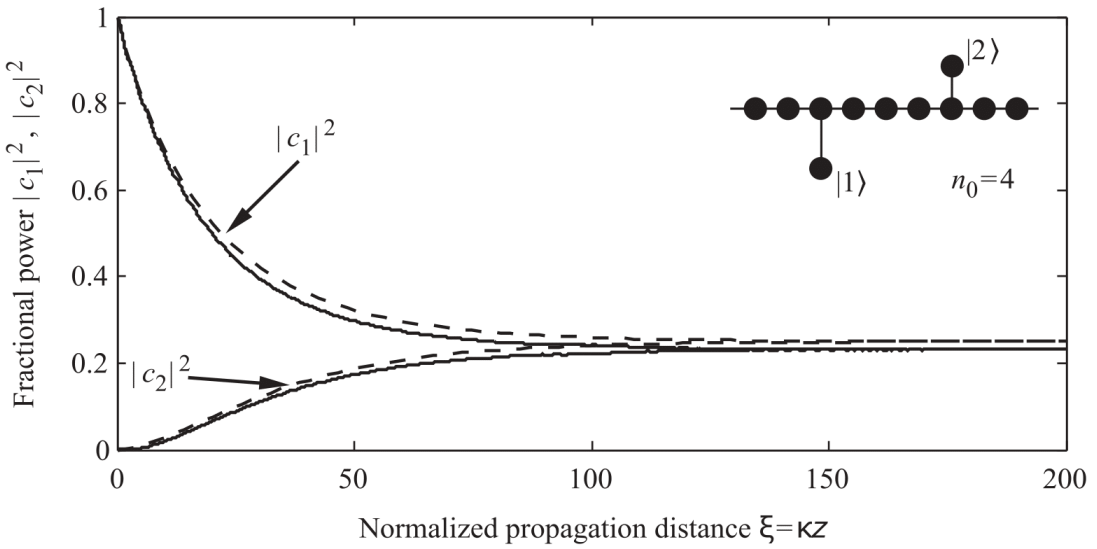

Figure 2.5: Fractional light power $|c_1|^2$ and $|c_2|^2$ in waveguide $|1\rangle$ and $|2\rangle$, respectively, versus normalized distance $\xi = \kappa z$, for the optical structure shown in the inset. Parameter values are: $\kappa_1/\kappa = \kappa_2/\kappa = 0.2$ and $\omega_1/\kappa = \omega_2/\kappa = 0$. Solid lines represent the numerically computed results, whereas the dashed ones are obtained from Eqns. (2.43) and (2.44), in the Markovian approximation. [7].

Under these last conditions, a "steady-state" solution ($z \to \infty$) for the coupled mode equations (2.4) and (2.5) can be written down

$$b_n = 0 \qquad \text{for } n < 0, \quad n > n_0, \quad n = 0,\, 2,\, 4,\, ...,\, n_0 \tag{2.47}$$

$$b_1 = -\frac{\kappa_1}{\kappa}, \quad b_3 = \frac{\kappa_1}{\kappa}, \quad b_5 = -\frac{\kappa_1}{\kappa}, \quad ..., \quad b_{n_0-1} = (-1)^{n_0/2}\frac{\kappa_1}{\kappa} \tag{2.48}$$

$$c_1 = 1, \quad c_2 = -(-1)^{n_0/2}\frac{\kappa_1}{\kappa_2} \tag{2.49}$$

All the waveguides in the array, with $n \leq 0$ and $n_0 \geq 0$, decouple from the other waveguides of the structure. This is made possible by the destructive interference of different tunneling paths. In fact, waveguides in the array at the position $n = 0$ and $n = n_0$ experience vanishing tunneling rates, $-\kappa b_1 - \kappa_1 c_1$ and $-\kappa b_{n_0-1} - \kappa_2 c_2$, respectively. This particular state is known as "dark mode state". This state can be use in an interesting way by changing very slowly, as compared to the characteristic time scale of the system, the ratio κ_1/κ_2, so that excitations can be transfered between the two side waveguides $|1\rangle$ and $|2\rangle$, thus using the waveguide lattice as a virtual bus.

On a final note we end the chapter by reporting that these kind of optical structures can be physically realized by focusing femtosecond laser pulses inside transparent materials, like glass [21,22]. The coupling constants κ and κ_α can be controlled by changing the distance between the waveguides. Different propagation constant mismatches ω_α are achieved by changing the writing speed.

Chapter 3

Particle statistics

We investigate the role of particle statistics in quantum decay processes in the presence of Fano resonances and BIC through the optical structures built in the previous chapter; in particular, the infinite array coupled to two side waveguides, the analogue of a two-level Fano-Anderson model. For now, we'll stay in the realm of quantum mechanics and use the same symbols of optics with the usual correlations. As before, propagation in space in optics is replaced by evolution in time in quantum mechanics.

As a starting approximation, we will completely disregard the interaction between the particles and focus on their bosonic or fermionic nature. The Fano-Anderson model describes a system of two discrete states $|1\rangle$ and $|2\rangle$, like in two quantum wells, and a common continuum, an infinite linear quantum wire. The tight-binding lattice band spans the energy interval $-2\hbar\kappa < E < 2\hbar\kappa$, where κ is the hopping rate between two adjacent sites of the quantum wire. The energy offsets, from the band center, of the two states, E_1 and E_2, are assumed, generally but not necessarily, to fall inside the continuum, i.e. $|E_1| < 2\hbar\kappa$ and $|E_2| < 2\hbar\kappa$. We assume again that the coupling between the states and the continuum is much weaker than the hopping rate, i.e. $\kappa_\alpha \ll \kappa$ for $\alpha = 1$ and 2.. To make apparent the nature of the particles, we need at least two of them. We place, at $t = 0$, one particle in state $|1\rangle$ and the other in state $|2\rangle$.To describe the quantum decay we introduce the survival probability

$$P_s(t) = |\langle\psi(0)|\psi(t)\rangle|^2 \tag{3.1}$$

This is clear. According to the rules of quantum mechanics, we are projecting the final state $|\psi(t)\rangle$ onto the initial state $|\psi(0)\rangle$ by taking the inner product between them, resulting in the probability amplitude that the state of the system, at a later time t, is still in the initial state, at $t = 0$. Taking the square of the modulus gives us the desired probability that, at time t, none of the two particles has decayed into the continuum. The Hamiltonian of the two-level Fano-Anderson model, in second quantization framework, can be written down immediately [8] from its "first-quantized" version already used in Eqn. (2.13)

$$\hat{H} = \sum_{n=1}^{2} E_n \hat{a}_n^\dagger \hat{a}_n + \int dk\, E(k)\hat{c}^\dagger(k)\hat{c}(k) + \sum_{n=1}^{2} \int dk \left[g_n(k)^* \hat{a}_n^\dagger \hat{c}(k) + g_n(k)\hat{c}^\dagger(k)\hat{a}_n \right] \tag{3.2}$$

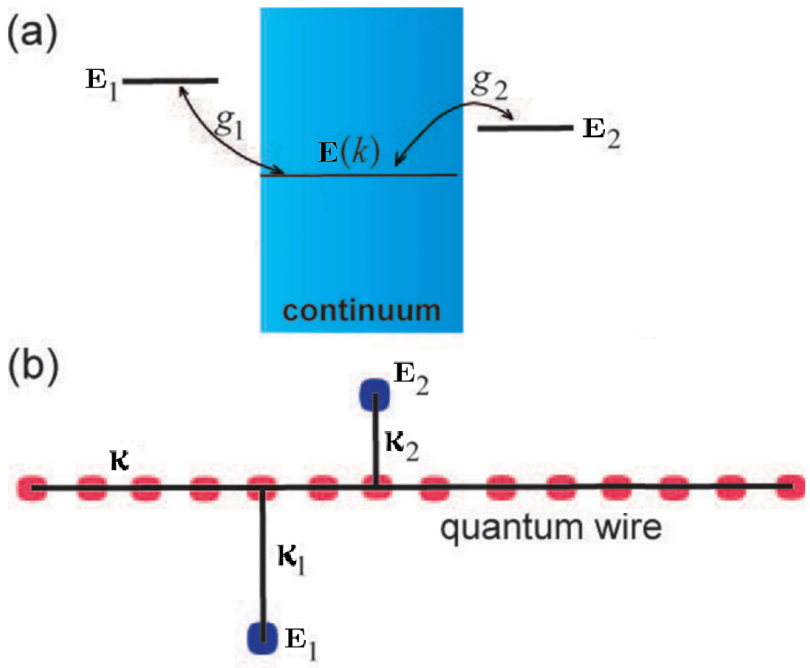

Figure 3.1: (a) Schematic of two discrete levels, of energy E_1 and E_2, coupled to a common continuum. (b) Physical realization of the two-level Fano-Anderson model based on two quantum wells side-coupled to a tight binding quantum wire, with hopping rates κ_1, κ_2 and κ. Adapted from [10].

where $\hat{a}_n$ and $\hat{a}_n^\dagger$ are the annihilation and creation operators, respectively, of particles at the discrete energy level E_n $(n = 1, 2)$, $\hat{c}(k)$ and $\hat{c}^\dagger(k)$ are the annihilation and creation operators, respectively, of particles at energy $E(k)$ in the continuum, and $g_n(k)$ is the spectral coupling function between the nth discrete level and the continuum; see Figure 3.1.
Creation and annihilation operators commute if they are associated with bosonic particles and anticommute for fermionic ones.

BOSONS — $\left[\hat{A}, \hat{B}\right]_- = \hat{A}\hat{B} - \hat{B}\hat{A}$

$$\left[\hat{a}_n, \hat{a}_m^\dagger\right]_- = \delta_{n,m} \tag{3.3}$$
$$\left[\hat{c}(k), \hat{c}^\dagger(k')\right]_- = \delta(k - k') \tag{3.4}$$
$$\text{All other commutators zero} \tag{3.5}$$

FERMIONS — $\left[\hat{A}, \hat{B}\right]_+ = \hat{A}\hat{B} + \hat{B}\hat{A}$

$$\left[\hat{a}_n, \hat{a}_m^\dagger\right]_+ = \delta_{n,m} \tag{3.6}$$
$$\left[\hat{c}(k), \hat{c}^\dagger(k')\right]_+ = \delta(k - k') \tag{3.7}$$
$$\text{All other anticommutators zero} \tag{3.8}$$

The particle number operator

$$\hat{N} = \sum_{n=1}^{2} \hat{a}_n^\dagger \hat{a}_n + \int dk\, \hat{c}^\dagger(k)\hat{c}(k) \tag{3.9}$$

commutes with the Hamiltonian, so, since it has no explicit time dependence, its eigenvalues G are constants of motion. G can only take non-negative integer values and is the number of particles in the system. The Hamiltonian, being a multi-particle operator, no longer acts on the simple Hilbert space $\mathcal{H}$ of single-particle quantum mechanics, but on Fock space $\mathcal{F}$, which is the space that includes an arbitrary number of particles. It can be expressed as the following direct sum

$$\mathcal{F} = \bigoplus_{G=0}^{\infty} \mathcal{F}_G \tag{3.10}$$

where $\mathcal{F}_0$ is the set containing only the vacuum state $|0\rangle$ (no particles), $\mathcal{F}_1$ is the usual single-particle Hilbert space and $\mathcal{F}_G$, for $G > 1$, is the symmetrized or antisymmetrized tensor product of $\mathcal{F}_1$, G times. Since the number of particles is constant, we will not jump between subspaces of $\mathcal{F}$ with different number of particles and so we can consider each subspace separately. For the case of one particle, $G = 1$, we are in the single-particle Hilbert space. The state vector can thus be expanded as

$$|\psi(t)\rangle = \sum_{n=1}^{2} A_n(t)\hat{a}_n^\dagger |0\rangle + \int dk\, \Upsilon(k,t)\hat{c}^\dagger(k) |0\rangle \tag{3.11}$$

where $A_n(t)$ and $\Upsilon(k,t)$ are the probability amplitudes to find the particle at the nth discrete level or in the continuum with wave number k, respectively. Everything is normalized

$$\sum_{n=1}^{2} |A_n(t)|^2 + \int dk\, |\Upsilon(k,t)|^2 = 1 \tag{3.12}$$

To find the time evolution of these probability amplitudes, we use the Schrödinger equation. Having assumed orthonormalization, such that $\langle n|n'\rangle = \delta_{n,n'}$, $\langle n|k\rangle = 0$ and $\langle k|k'\rangle = \delta(k-k')$, using the appropriate commutation relations to put the operators in normal order (creation to the left, annihilation to the right) and remembering that $\hat{a}_n |0\rangle = 0$ and $\hat{c}_n |0\rangle = 0$, we get the following equations

$$\begin{cases} i\dfrac{\partial}{\partial t} A_n(t) = E_n A_n + \displaystyle\int dk\, g_n^*(k)\Upsilon(k,t) & (3.13) \\ i\dfrac{\partial}{\partial t}\Upsilon(k,t) = E(k)\Upsilon(k,t) + \displaystyle\sum_{n=1}^{2} g_n(k)A_n(t) & (3.14) \end{cases}$$

The result is independent of the bosonic or fermionic nature of the particle, as it should, since there's only one particle. Following the same procedure in Chapter 2, the continuum degree of freedom $\Upsilon(k,t)$ is eliminated in Eqns. (3.13) and (3.14). In

the Markovian approximation, the time evolution of the discrete degrees of freedom is

$$\frac{\partial}{\partial t}A_n(t) = \sum_{n=1}^{2} M_{n,m}A_m \tag{3.15}$$

where the elements of the complex-valued 2 x 2 matrix $\mathcal{M}$ are given by

$$M_{n,m} = -iE_n\delta_{n,m} - \int_0^\infty d\tau\, \Phi_{n,m}(\tau)\exp\Big(\frac{iE_m\tau}{\hbar}\Big) \tag{3.16}$$

with

$$\Phi_{n,m}(\tau) = \int dk\, g_n^*(k)g_m(k)\exp\Big(-\frac{iE(k)\tau}{\hbar}\Big) \tag{3.17}$$

Let's assume now that the particle starts in one of the two discrete levels, say n_0, at time $t = 0$, i.e. $A_n(0) = \delta_{n,n_0}$ and $\Upsilon(k, 0) = 0$. We call $S_{n,n_0}(t)$ and $S_{n_0}(k, t)$ the solutions $A_n(t)$ and $\Upsilon(k, t)$ to the system of Eqns. (3.13) and (3.14), respectively, under these initial conditions. Then this is the solution to the system Eqn. (3.15), given by the exponential matrix

$$\mathcal{S} = \exp(\mathcal{M}t) \tag{3.18}$$

a 2 x 2 matrix with elements $S_{n,n_0}(t)$. The probability amplitude for the particle to be in the nth bare discrete level at time t, when at time $t = 0$ it was in the same discrete level, is simply $S_{n,n}(t)$ and if we want the probability, we just take the modulus and square it.
Now we move to the interesting case of two particles. We are now in the symmetrized (bosons) or antisymmetrized (fermions) part of $\mathcal{F}_1 \otimes \mathcal{F}_1$. Both particles are placed, at $t = 0$, in the (bare) discrete levels, one per level. The initial state is then

$$|\psi(0)\rangle = \hat{a}_1^\dagger\hat{a}_2^\dagger\,|0\rangle \tag{3.19}$$

Note that, for the case of non-interacting bosons, this is not the lowest energy state of the system, since every boson should be placed in the lowest discrete level. The vector state $|\psi(t)\rangle$ is obtain by the formal replacement

$$\hat{a}_l^\dagger \to \sum_{n=1}^{2} S_{n,l}(t)\hat{a}_n^\dagger + \int dk\, S_l(k, t)\hat{c}^\dagger(k) \tag{3.20}$$

This is reasonable since all the governing equations are linear and so the whole system is linear. We are simply propagating in time each part of the system through all possible routes, in pure Feynman's style. In fact, for this reason the quantities $S_{n,l}(t)$ and $S_l(k, t)$ are called propagators. We have then

$$|\psi(t)\rangle = \left[\prod_{l=1}^{2}\left(\sum_{n=1}^{2} S_{n,l}(t)\hat{a}_n^\dagger + \int dk\, S_l(k, t)\hat{c}^\dagger(k)\right)\right]|0\rangle \tag{3.21}$$

where $S_{n,l}(t)$ and $S_l(k, t)$ are the solutions $A_n(t)$ and $\Upsilon(k, t)$ to the system of Eqns. (3.13) and (3.14) for the single particle with initial conditions $A_n(0) = \delta_{n,l}$ and

$\Upsilon(k,0)=0$. The survival probability $P_s(t)=|\langle\psi(0)|\psi(t)\rangle|^2$ can be easily calculated for bosons and fermions, using the correct commutation relations. To simplify a bit the expression, we do not include all the terms associated with the continuum degrees of freedom because they vanish. In fact there is always an annihilation operator of the discrete degrees of freedom that goes through to the right, thus acting on the vacuum. We have then

$$\begin{aligned}
&\langle\psi(0)|\psi(t)\rangle = \\
&= \langle 0|\,\hat{a}_2\hat{a}_1\Big(S_{1,1}(t)\hat{a}_1^\dagger + S_{2,1}(t)\hat{a}_2^\dagger\Big)\Big(S_{1,2}(t)\hat{a}_1^\dagger + S_{2,2}(t)\hat{a}_2^\dagger\Big)\,|0\rangle \\
&= \langle 0|\,\hat{a}_2\hat{a}_1\Big(S_{1,1}(t)S_{1,2}(t)\hat{a}_1^\dagger\hat{a}_1^\dagger + S_{1,1}(t)S_{2,2}(t)\hat{a}_1^\dagger\hat{a}_2^\dagger \\
&\qquad + S_{2,1}(t)S_{1,2}(t)\hat{a}_2^\dagger\hat{a}_1^\dagger + S_{2,1}(t)S_{2,2}(t)\hat{a}_2^\dagger\hat{a}_2^\dagger\Big)\,|0\rangle \\
&= \langle 0|\,\hat{a}_2\hat{a}_1\Big(S_{1,1}(t)S_{2,2}(t)\hat{a}_1^\dagger\hat{a}_2^\dagger + S_{2,1}(t)S_{1,2}(t)\hat{a}_2^\dagger\hat{a}_1^\dagger\Big)\,|0\rangle \\
&= \langle 0|\,\hat{a}_2\hat{a}_1\Big(S_{1,1}(t)S_{2,2}(t) \pm S_{2,1}(t)S_{1,2}(t)\Big)\hat{a}_1^\dagger\hat{a}_2^\dagger\,|0\rangle \\
&= \langle 0|\,\Big(S_{1,1}(t)S_{2,2}(t) \pm S_{2,1}(t)S_{1,2}(t)\Big)\Big(\pm\hat{a}_1^\dagger\hat{a}_1 + 1\Big)\Big(\pm\hat{a}_2^\dagger\hat{a}_2 + 1\Big)\,|0\rangle \\
&= S_{1,1}(t)(S_{2,2}(t) \pm S_{2,1}(t)(S_{1,2}(t)
\end{aligned} \tag{3.22}$$

where the plus sign is for bosons and the minus sign for fermions. The survival probabilities are then

$$P_s^{(bos)}(t) = |S_{1,1}S_{2,2} + S_{2,1}S_{1,2}|^2 = |\mathrm{perm}\,\mathcal{S}| \tag{3.23}$$

$$P_s^{(ferm)}(t) = |S_{1,1}S_{2,2} - S_{2,1}S_{1,2}|^2 = |\det\mathcal{S}| \tag{3.24}$$

Having discussed the two-level Fano-Anderson model in the second-quantization framework, we now move to the optical realm and simulate the decay process of two indistinguishable particles, mapping time evolution to space propagation.
To simulate the particles we produce two polarization-entangled photons and launch them into the two side waveguides, one in each waveguide. Let us call $\hat{a}_{n,T}^\dagger$ the creation operator of photons in the fundamental mode of waveguide $|n\rangle$ with polarization states $T=H$ (horizontal) or $T=V$ (vertical), respectively. The wave function of the two entangled photons, injected in the waveguides $|1\rangle$ and $|2\rangle$ at the plane $z=0$, is

$$|\psi(z=0)\rangle = \frac{1}{\sqrt{2}}\big(\hat{a}_{1,H}^\dagger\hat{a}_{2,V}^\dagger + e^{i\varphi}\hat{a}_{1,V}^\dagger\hat{a}_{2,H}^\dagger\big)\,|0\rangle \tag{3.25}$$

The phase φ is an adjustable parameter allowing us to simulate, as we'll sew, both bosons, for $\varphi=0$, and fermions, for $\varphi=\pi$. To calculate the state of the two photon in the optical structure at a generic position z, we just formally make the following substitution into Eqn. (3.25), as explained in [9] for linear optical systems

$$\hat{a}_{n,T}^\dagger \to \sum_{j=1}^{\infty} S_{j,n}^{(T)}(z)\hat{a}_{j,T}^\dagger \tag{3.26}$$

where $S_{j,n}^{(T)}(z)$ is the amplitude probability that one photon with polarization T, injected at $z = 0$ in the waveguide $|n\rangle$, is found in the waveguide $|j\rangle$ after a propagation length z. This amplitude can be calculated from classical coupled-mode theory describing propagation of (classical) light in the particular optical structure. We obtain

$$\begin{aligned}|\psi(z)\rangle = \frac{1}{\sqrt{2}}\Bigg(&\sum_{j=1}^{\infty} S_{j,1}^{(H)}(z)\hat{a}_{j,H}^{\dagger} \sum_{j=1}^{\infty} S_{j,2}^{(V)}(z)\hat{a}_{j,V}^{\dagger} \\ &+ e^{i\varphi}\sum_{j=1}^{\infty} S_{j,1}^{(V)}(z)\hat{a}_{j,V}^{\dagger} \sum_{j=1}^{\infty} S_{j,2}^{(H)}(z)\hat{a}_{j,H}^{\dagger}\Bigg)|0\rangle\end{aligned} \tag{3.27}$$

Using the fact that photons are bosons, so the creation and annihilation operators commute, we find

$$\begin{aligned}|\psi(z)\rangle = \frac{1}{\sqrt{2}}\Big[&\Big(S_{1,1}^{(H)}S_{1,2}^{(V)} + e^{i\varphi}S_{1,1}^{(V)}S_{1,2}^{(H)}\Big)\hat{a}_{1,H}^{\dagger}\hat{a}_{1,V}^{\dagger} \\ &+ \Big(S_{1,1}^{(H)}S_{2,2}^{(V)} + e^{i\varphi}S_{2,1}^{(V)}S_{1,2}^{(H)}\Big)\hat{a}_{1,H}^{\dagger}\hat{a}_{2,V}^{\dagger} \\ &+ \Big(S_{2,1}^{(H)}S_{1,2}^{(V)} + e^{i\varphi}S_{1,1}^{(V)}S_{2,2}^{(H)}\Big)\hat{a}_{2,H}^{\dagger}\hat{a}_{1,V}^{\dagger} \\ &+ \Big(S_{2,1}^{(H)}S_{2,2}^{(V)} + e^{i\varphi}S_{2,1}^{(V)}S_{2,2}^{(H)}\Big)\hat{a}_{2,H}^{\dagger}\hat{a}_{2,V}^{\dagger} \\ &+ \dots\Big]|0\rangle\end{aligned} \tag{3.28}$$

where we have not written down the terms not interesting to us, meaning those with operators' products $\hat{a}_{j,H}^{\dagger}\hat{a}_{n,V}^{\dagger}$ with either $j > 2$ or $n > 2$. The coincidence probability $P^{(1,1)}(z)$ to find one photon, after a propagation z, in waveguide $|1\rangle$ with polarization H and the other photon in waveguide $|2\rangle$ with polarization V or to find one photon in waveguide $|2\rangle$ with polarization H and the other photon in waveguide $|1\rangle$ with polarization V, assuming that the amplitude probabilities $S_{n,j}^{(T)}$ (for $n, j = 1, 2$) do not depend on the polarization state, i.e. $S_{n,j}^{(H)} = S_{n,j}^{(V)} \equiv S_{n,j}$ is immediately readable from Eqn. (3.28)

$$\begin{aligned}P^{(1,1)}(z) = &\frac{1}{2}\left|S_{1,1}S_{2,2} + e^{i\varphi}S_{2,1}S_{1,2}\right|^2 \\ &+ \frac{1}{2}\left|S_{2,1}S_{1,2} + e^{i\varphi}S_{1,1}S_{2,2}\right|^2\end{aligned} \tag{3.29}$$

For $\varphi = 0$ and for $\varphi = \pi$ the coincidence probability has exactly the same functional form as the survival probability we have found in Fano-Anderson model for bosons and for fermions, respectively. We will then just call it the survival probability. We compare this probability with the result for two distinguishable particles: we neglect the quantum interference by summing the square moduli of each four probability amplitudes giving distinguishable results, when each particle can be identified

$$P^{(dis)}(z) = |S_{1,1}S_{2,2}|^2 + |S_{2,1}S_{1,2}|^2 \tag{3.30}$$

We set $\hbar = 1$ and call propagation distance as t and no longer as z. With that, the energies of the bare discrete levels in the Fano-Anderson model correspond

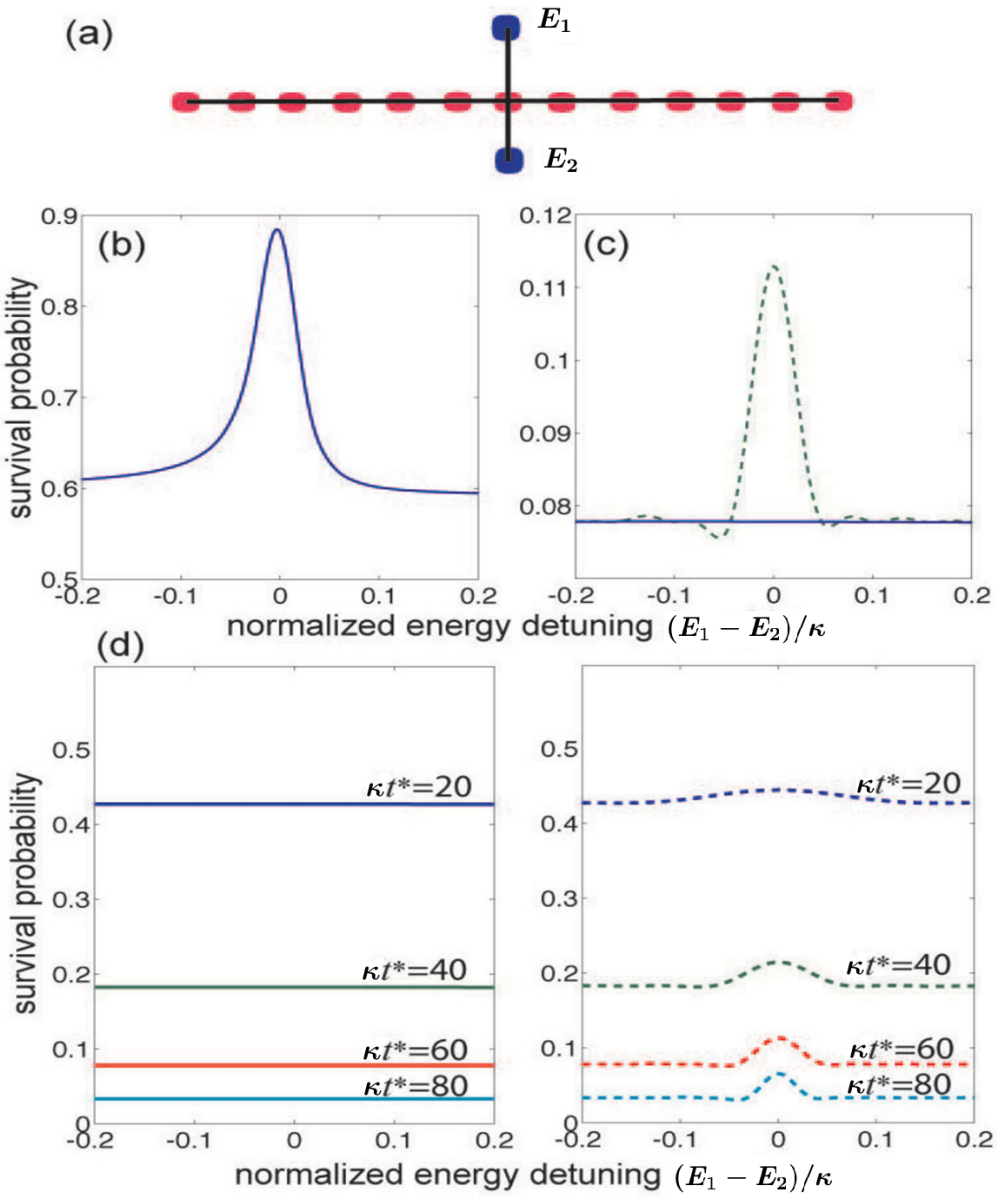

Figure 3.2: (a) Optical structure made up of two waveguides, marked by their propagation constant mismatches E_1 and E_2, side-coupled to an infinite waveguide array, analogue to two quantum wells coupled to a quantum wire. Parameter values are: $\kappa_1/\kappa = 0.05$, $\kappa_2/\kappa = 0.2$ and $E_2/\kappa = 0.1$ (b) Survival probability of a single photon versus normalized detuning $(E_2 - E_1)/\kappa$ at fixed distance $t^* = 200/\kappa$. The usual asymmetric Fano resonance around $E_1 = E_2$ is evident. (c) Survival probability versus normalized detuning $(E_2 - E_1)/\kappa$ at distance $t^* = 60/\kappa$, for two polarization-entangled photons, launched simultaneously one per side waveguide, in antisymmetric configuration, corresponding to $\varphi = \pi$ (solid line) and symmetric configuration, corresponding to $\varphi = 0$ (dashed line), simulating the evolution in time of two non-interacting fermions and bosons, respectively. (d) Dependence of the Fano resonance curves on the observation distance t^* for photons in antisymmetric configuration (left panel) and symmetric configuration (right panel). Adapted from [10].

to the propagation constants mismatches between the side waveguides and the waveguides in the array. κ, κ_1 and κ_2 are the hopping or coupling rates. The variable t represents time or space according to the context in which it's used.
Consider the structure in Figure 3.2(a). We can analyze this structure ([10]) as we did in Chapter 2, by launching light into one of the two side waveguides. The survival probability is plotted versus normalized detuning $(E_1 - E_2)/\kappa$ in Figure 3.2(b), where, at a fixed distance, we see, around $E_1 = E_2$, a Fano resonance with the typical asymmetric shape. We now launch two polarization-entangled photons, one per side waveguide, in the symmetric (bosonic) and antisymmetric (fermionic) state. In Figure 3.2(c) we see, in dashed line, the bosonic case, with again the Fano resonance. For fermions, in solid line, something new happens: a complete suppression of Fano resonance. Such a result is independent of the distance we observe the phenomenon; Figure 3.2(d) shows this fact by plotting the survival probability, for fermions (left picture, solid line) and bosons (right picture, dashed line), at various distances. We interpret these results as the action of Pauli exclusion principle: two fermions, unlike two bosons, cannot occupy the same level (they cannot be in the same state) and so one of them, having no place to go, must decay away into the continuous states. To put this model to the test, we will consider now a different structure, a semi-infinite array of evanescently coupled waveguides, side-coupled with two waveguides at the first element of the array, as shown in Figure 3.3(b) and 3.3(e). The coupled-mode equations that govern the system, following [14], can be written in Bloch basis $|k\rangle$, where $0 \leq k \leq \pi$, as

$$\begin{cases} i\dfrac{dc}{dt} = E(k)c(k,t) + \displaystyle\sum_{\alpha=1}^{2} v_\alpha(k)c_\alpha(t) & (3.31) \\ i\dfrac{dc_\alpha}{dt} = E_\alpha c_\alpha(t) + \displaystyle\int_0^\pi dk\, v_\alpha(k)c(k,t) \qquad (\alpha = 1,\, 2) & (3.32) \end{cases}$$

with

$$E(k) = -2\kappa\cos k \quad , \quad v_\alpha = \sqrt{\frac{2}{\pi}}\kappa_\alpha \sin k \tag{3.33}$$

Everything else has the same meaning as in Eqns. (2.10) and (2.11), with the following correspondences: $t \leftrightarrow z$, $E_\alpha \leftrightarrow \omega_\alpha$, $E(k) = \omega(k) = -2\kappa\cos k$.
Due to the range of k, we can expand the amplitude $c(k,t)$ in a Fourier series of sine terms only

$$c(k,t) = -\sqrt{\frac{2}{\pi}}\sum_{n=1}^{\infty} b_n(t)\sin(nk) \tag{3.34}$$

Upon substitution, starting first from Eqn. (3.31), we obtain

$$-i\sqrt{\frac{2}{\pi}}\sum_{n=1}^{\infty}\frac{db_n}{dt}\sin(nk) = 2\kappa\cos k\sqrt{\frac{2}{\pi}}\sum_{n=1}^{\infty} b_n\sin(nk) + \sqrt{\frac{2}{\pi}}\sum_{\alpha=1}^{2}\kappa_\alpha c_\alpha(t)\sin k \tag{3.35}$$

Multiplying both sides by $\sin(mk)$, integrating over k and using the following relation

$$\int_0^\pi dk\, \sin(nk)\sin(mk) = \frac{\pi}{2}\delta_{n,m} \tag{3.36}$$

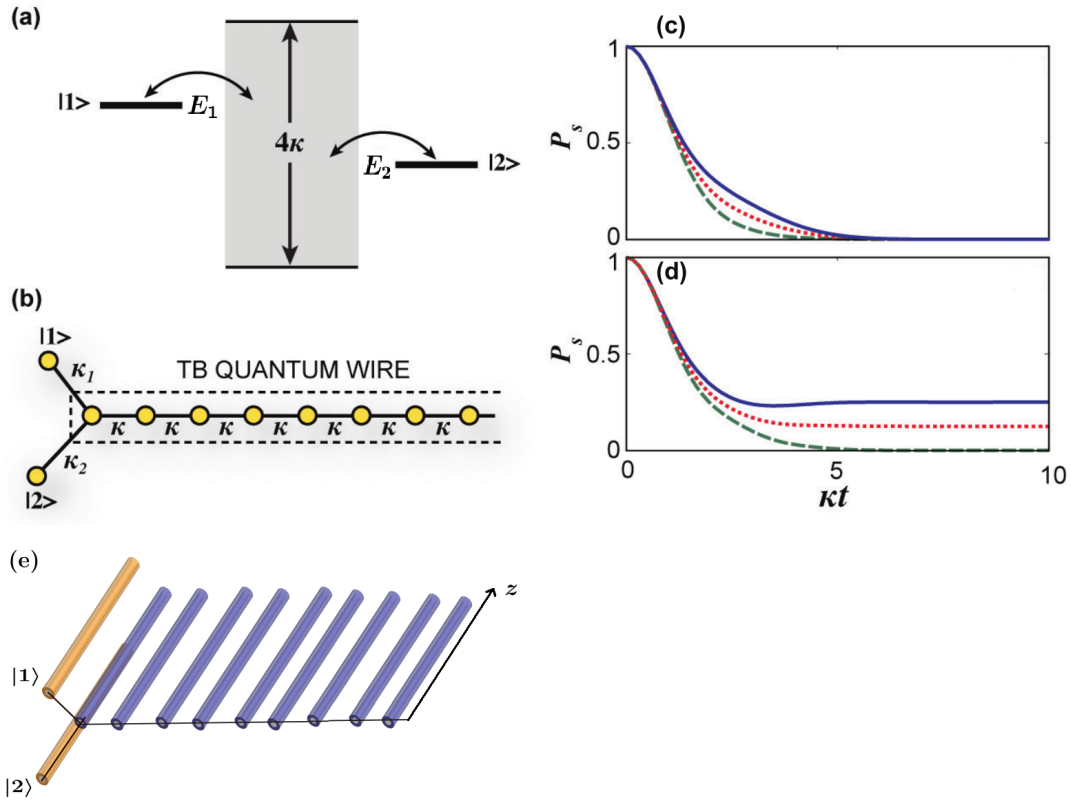

Figure 3.3: (a) Schematic of two discrete levels, of energy E_1 and E_2, coupled to a common continuum, spanning the energy band of width 4κ ($\hbar = 1$). (b) Physical realization of the two-level Fano-Anderson model based on two quantum wells side-coupled to a tight binding semi-infinite quantum wire, with hopping rates κ_1, κ_2 and κ. (e) Photonic structure simulating the model in (a). Quantum wells are replaced by side-coupled waveguides and the quantum wire by a semi-infinite array of evanescently coupled waveguides. (c,d) Survival probability, versus normalized distance κt, for two polarization-entangled photons, launched simultaneously one per side waveguide, in antisymmetric configuration, corresponding to $\varphi = \pi$ (dashed line), and symmetric configuration, corresponding to $\varphi = 0$ (solid line), which simulate the evolution in time of the survival probability for two non-interacting fermions and bosons, respectively. Distinguishable photons, simulating distinguishable non-interacting particles, are also considered, shown in dotted curves. Parameter values are: $\kappa_1/\kappa = \kappa_2/\kappa = 0.5$. $E_1/\kappa = 0$, $E_2/\kappa = 0.8$ for (c). $E_1/\kappa = E_2/\kappa = 0.8$ for (d).

where m is a positive integer, we get

$$-i\frac{db_m}{dt} = \frac{2}{\pi}\int_0^\pi 2\kappa\cos k\sin(mk)\sum_{n=1}^{\infty} b_n sin(nk)dk + \sum_{\alpha=1}^{2}\kappa_\alpha c_\alpha(t)\delta_{m,1} \tag{3.37}$$

For $m = 1$

$$\begin{aligned} -i\frac{db_1}{dt} &= \frac{2}{\pi}\int_0^\pi 2\kappa\cos k\sin k\sum_{n=1}^{\infty} b_n sin(nk)dk + \sum_{\alpha=1}^{2}\kappa_\alpha c_\alpha(t) \\ &= \frac{2}{\pi}\sum_{n=1}^{\infty} b_n\int_0^\pi \kappa\sin(2k)sin(nk)dk + \sum_{\alpha=1}^{2}\kappa_\alpha c_\alpha(t) \\ &= \frac{2}{\pi}\sum_{n=1}^{\infty} b_n\kappa\frac{\pi}{2}\delta_{2,n} + \sum_{\alpha=1}^{2}\kappa_\alpha c_\alpha(t) \\ &= \kappa b_2 + \kappa_1 c_1 + \kappa_2 c_2 \end{aligned} \tag{3.38}$$

For $m > 1$

$$\begin{aligned} -i\frac{db_m}{dt} &= \sum_{n=1}^{\infty}\frac{4\kappa}{\pi}b_n\int_0^\pi cosk\sin(mk)sin(nk)dk + \sum_{\alpha=1}^{2}\kappa_\alpha c_\alpha(t) \\ &= \sum_{n=1}^{\infty}\frac{4\kappa}{\pi}b_n\int_0^\pi \frac{1}{2}[\sin(m+1)k + \sin(m-1)k]sin(nk)dk + \sum_{\alpha=1}^{2}\kappa_\alpha c_\alpha(t) \\ &= \sum_{n=1}^{\infty}\kappa b_n(\delta_{n,m+1} + \delta_{n,m-1}) + \sum_{\alpha=1}^{2}\kappa_\alpha c_\alpha(t) \\ &= \kappa(b_{m+1} + b_{m-1}) + \kappa_1 c_1 + \kappa_2 c_2 \end{aligned} \tag{3.39}$$

Moving on to Eqn. (3.32)

$$\begin{aligned} i\frac{dc_\alpha}{dt} &= E_\alpha c_\alpha - \frac{2}{\pi}\kappa_\alpha\sum_{n=1}^{\infty} b_n\int_0^\pi \sin k\sin(nk)dk \\ &= E_\alpha c_\alpha - \kappa_\alpha\sum_{n=1}^{\infty} b_n\delta_{1,n} \\ &= E_\alpha c_\alpha - \kappa_\alpha b_1 \qquad\qquad (\alpha = 1,\ 2) \end{aligned} \tag{3.40}$$

Putting everything together, we have the dynamic system in Wannier basis

$$\begin{cases} i\dfrac{db_1}{dt} = -\kappa b_2 - \kappa_1 c_1 - \kappa_2 c_2 & (3.41) \\ i\dfrac{db_n}{dt} = -\kappa(b_{n+1} + b_{n-1}) & (3.42) \\ i\dfrac{dc_1}{dt} = -\kappa_1 b_1 + E_1 c_1 & (3.43) \\ i\dfrac{dc_2}{dt} = -\kappa_2 b_1 + E_2 c_2 & (3.44) \end{cases}$$

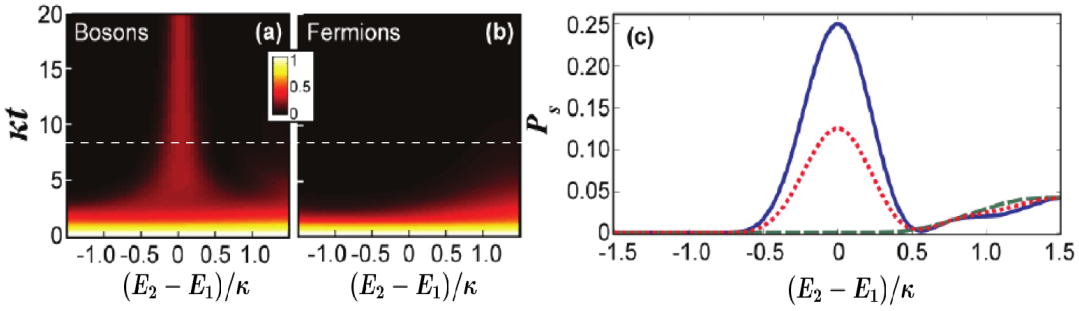

Figure 3.4: Map of the survival probability P_s as a function of κt and $(E_2 - E_1)/\kappa$ for (a) bosons, and (b) fermions. Parameter values are: $\kappa_1/\kappa = \kappa_2/\kappa = 0.5$ and $E_1/\kappa = 0.8$ (Fano interference regime). In (c) the behavior of P_s versus $(E_2 - E_1)/\kappa$ is shown at the normalized time $t = 8/\kappa$ for bosons (solid curve), fermions (dashed curve) and for distinguishable particles (dotted curve).

where n is a positive integer starting from 1 and labeling the waveguides in the array. This dynamic system describes exactly the structure in Figure 3.3(b,e). The waveguide corresponding to $n = 1$ is the one coupled to the two side waveguides $|1\rangle$ and $|2\rangle$; everything else has the same meaning as in Eqns. (2.4) and (2.5), with $t \leftrightarrow z$. Performing an analogue analysis as we did for the previous structure (Figure 3.2(a)), we obtain a similar response, shown in Figure 3.3(c), where the survival probability has been plotted versus time, for parameter values $\kappa_1/\kappa = \kappa_2/\kappa = 0.5$, $E_1/\kappa = 0$ and $E_2/\kappa = 0.8$. An analysis for single particles placed in waveguide $|1\rangle$ or $|2\rangle$, for the same parameters, shows complete decay, no BIC. Placing two particles, we have again complete decay, being faster for fermions (dashed line) than bosons (solid line). An intermediate behavior is seen for distinguishable particles (dotted line). At resonance, for $E_1/\kappa = E_2/\kappa = 0.8$, we see, in Figure 3.3(d), fractional (not complete) decay for bosons and distinguishable particles, owing to the existence of a BIC at $E = E_1 = E_2$. Fermions show complete decay. To highlight what happens at this resonance, the survival probability is plotted, in Figure 3.4(c) versus normalized propagation constant mismatch $(E_2 - E_1)/\kappa$ at fixed normalized distance of $t = 8/\kappa$, for bosons (solid line), fermions (dashed line) and distinguishable particles (dotted line), at parameter values $\kappa_1/\kappa = \kappa_2/\kappa = 0.5$ and $E_1/\kappa = 0.8$. We see, for fermions, complete suppression of Fano resonance. A combined graph of these results is shown in Figure 3.4(a) for bosons and (b) for fermions. An actual experiment [11] has been done to verify these theoretical results and everything works out as predicted.

A different scenario is revealed if we consider the energy levels E_1 and E_2 outside the continuous band. In this case, the Fano-Anderson model allows the existence of two bound dressed states *outside* the continuum. One particle, placed in level $|1\rangle$ or $|2\rangle$, will show fractional decay and Rabi-like oscillations when E_1 is close to E_2. Figure 3.5 shows the behavior for two particles with parameter values $\kappa_1/\kappa = \kappa_2/\kappa = 0.5$ and $E_1 = 4\kappa$. Now that we have two dressed levels available, fermions can be placed in each level without violating Pauli exclusion principle. The survival probability is plotted versus time at $E_1 = E_2 = 4\kappa$ in Figure 3.5(d)

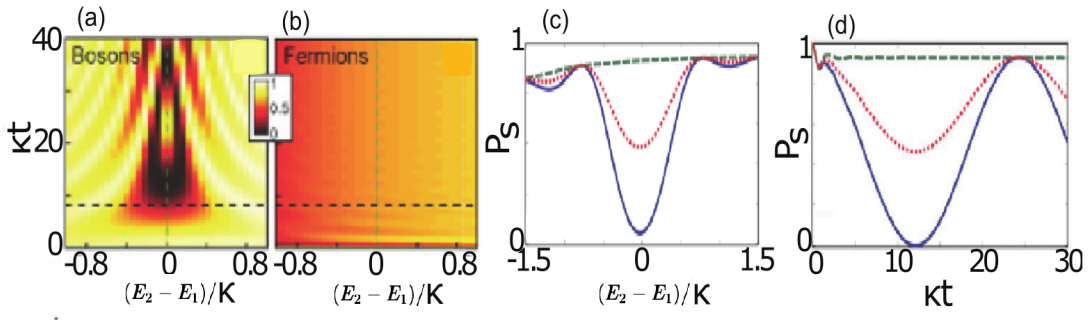

Figure 3.5: Map of the survival probability P_s as a function of κt and $(E_2 - E_1)/\kappa$ for (a) bosons, and (b) fermions. Parameter values are: $\kappa_1/\kappa = \kappa_2/\kappa = 0.5$ and $E_1/\kappa = 4$ (Rabi oscillations regime). In (c) the behavior of P_s versus $(E_2 - E_1)/\kappa$ at time $t = 8/\kappa$ is shown, whereas in (d) P_s is plotted versus κt for $E_2 = E_1$. Solid curves: bosons; dashed curves: fermions; dotted curves: distinguishable particles.

where fractional decay is observed for fermions (dashed line) while for bosons (solid line) Rabi oscillations emerge. No Rabi oscillations for fermions. An intermediate behavior for distinguishable particle (dotted line) is also shown. A plot of the survival probability versus energy difference at fixed time $t = 8/\kappa$ is shown in Figure 3.5(c) and a combined plot in Figure 3.5(a). A simple analysis can be performed, following [15], for the two-particle case if we assume that (i) the energies E_1 and E_2 of the two levels $|1\rangle$ and $|2\rangle$ are far outside the continuous band, which means $|E(k) - E_{1,2}| \gg \kappa$ for every possible value of k; (ii) $|E(k) - E_{1,2}| \gg \kappa_{1,2}$ for every possible value of k; (iii) the detuning $|E_1 - E_2|$ is small, meaning of the same order or smaller than $\sim \kappa_1^2/E_1$; (iv) the coupling constants κ_1 and κ_2 are of the same order of magnitude.
Starting from the governing system in Bloch basis (Eqns. (3.31) and (3.32)), we make the following substitutions

$$c_\alpha(t) = f_\alpha(t)e^{-i\bar{E}t} \tag{3.45}$$

$$c(k,t) = f(k,t)e^{-i\bar{E}t} \tag{3.46}$$

where

$$\bar{E} \equiv \frac{(E_1 + E_2)}{2} + \frac{\kappa_1^2 + \kappa_2^2}{E_1 + E_2} \tag{3.47}$$

We get from Eqn. (3.31)

$$i\frac{df}{dt} = (E(k) - \bar{E})f + v_1 f_1 + v_2 f_2 \tag{3.48}$$

Since at time $t = 0$ there are no particles in the continuous band (no light is launched into the array), then $f(k,0) = 0$. Also, by assumption, $v_{1,2} \ll \left|E(k) - \bar{E}\right|$. It follows that $f(k,t)$ remains small, and at leading order we can neglect the time derivative in Eqn.(3.48), obtaining

$$f(k,t) \simeq \frac{v_1 f_1 + v_2 f_2}{\bar{E} - E} \tag{3.49}$$

Substituting this result in Eqns. (3.32) we get

$$\begin{cases} i\dfrac{df_1}{dt} \simeq f_1\left(E_1 - \bar{E} + \displaystyle\int_0^\pi dk\, \frac{v_1^2}{\bar{E} - E}\right) + f_2 \displaystyle\int_0^\pi dk\, \frac{v_1 v_2}{\bar{E} - E} & (3.50) \\ i\dfrac{df_2}{dt} \simeq f_1 \displaystyle\int_0^\pi dk\, \frac{v_1 v_2}{\bar{E} - E} + f_2\left(E_2 - \bar{E} + \displaystyle\int_0^\pi dk\, \frac{v_2^2}{\bar{E} - E}\right) & (3.51) \end{cases}$$

By the assumptions, we can approximate the integrals as

$$\int_0^\pi dk\, \frac{\sin^2 k}{\bar{E} + 2\kappa \cos k} \simeq \int_0^\pi dk\, \frac{\sin^2 k}{\bar{E}} = \frac{\pi}{2\bar{E}} \tag{3.52}$$

which, substituted into the system together with the definition of $\bar{E}$, gives

$$\begin{cases} i\dfrac{df_1}{dt} \simeq f_1\Big(\dfrac{E_1 - E_2}{2} + \dfrac{2\kappa_1^2}{\bar{E}} - \dfrac{\kappa_1^2 + \kappa_2^2}{E_1 + E_2}\Big) + f_2 \dfrac{2\kappa_1 \kappa_2}{\bar{E}} & (3.53) \\ i\dfrac{df_2}{dt} \simeq f_1 \dfrac{2\kappa_1 \kappa_2}{\bar{E}} + f_2\Big(\dfrac{E_2 - E_1}{2} + \dfrac{2\kappa_2^2}{\bar{E}} - \dfrac{\kappa_1^2 + \kappa_2^2}{E_1 + E_2}\Big) & (3.54) \end{cases}$$

The assumptions allow us to approximate $\bar{E}$ in the denominators with $E_1 + E_2 \simeq 2E_1$

$$\begin{cases} i\dfrac{df_1}{dt} \simeq f_1\Big(\dfrac{E_1 - E_2}{2} + \dfrac{\kappa_1^2 - \kappa_2^2}{2E_1}\Big) + f_2 \dfrac{\kappa_1 \kappa_2}{E_1} & (3.55) \\ i\dfrac{df_2}{dt} \simeq f_1 \dfrac{\kappa_1 \kappa_2}{E_1} + f_2\Big(\dfrac{E_2 - E_1}{2} + \dfrac{\kappa_2^2 - \kappa_1^2}{2E_1}\Big) & (3.56) \end{cases}$$

To put it more neatly, we rewrite the system in exact form

$$\begin{cases} i\dfrac{df_1}{dt} = -\Delta f_1 + + \kappa_e f_2 & (3.57) \\ i\dfrac{df_2}{dt} = \kappa_e f_1 + \Delta f_2 & (3.58) \end{cases}$$

where

$$\kappa_e \equiv \frac{\kappa_1 \kappa_2}{E_1} \qquad \Delta \equiv \frac{E_2 - E_1}{2} + \frac{\kappa_2^2 - \kappa_1^2}{2E_1} \tag{3.59}$$

The elements of the matrix $\mathcal{S}$ can be easily found. The meaning of $S_{1,1}(t)$ is the probability amplitude to be in state $|1\rangle$ at time t when, at $t = 0$, the state was $|1\rangle$. Since we have removed from the dynamics the continuous band, a general state can be approximately written as

$$|\psi(t)\rangle = f_1(t)\,|1\rangle + f_2(t)\,|2\rangle \tag{3.60}$$

From Eqn. (3.58) we have

$$f_1 = \frac{1}{\kappa_e}\Big(i\frac{df_2}{dt} - \Delta f_2\Big) \tag{3.61}$$

Substituting this into Eqn.(3.57) we obtain

$$-\frac{d^2 f_2}{dt^2} - i\Delta\frac{df_2}{dt} = \kappa_e^2 f_2 - i\Delta\frac{dc_2}{dt} + \Delta^2 f_2$$
$$\frac{d^2 f_2}{dt^2} = -(\kappa_e^2 + \Delta^2) f_2$$

The general solution for $f_2(t)$ is

$$f_2(t) = A\exp(i\sqrt{\kappa_e^2 + \Delta^2}t) + B\exp(-i\sqrt{\kappa_e^2 + \Delta^2}t) \tag{3.62}$$

The initial conditions, for $S_{1,1}$, are $f_1(0) = 1$ and $f_2(0) = 0$. From Eqn. (3.62) we immediately get $B = -A$. So

$$f_2(t) = 2iA\sin(\Omega t) \tag{3.63}$$

where $\Omega \equiv \sqrt{\kappa_e^2 + \Delta^2}$. Solving for $f_1(t)$

$$f_1(t) = \frac{2iA}{\kappa_e}(i\Omega\cos(\Omega t) - \Delta\sin(\Omega t)) \tag{3.64}$$

Using the other initial condition, $f_1(0) = 1$, we have

$$A = -\frac{\kappa_e}{2\Omega} \tag{3.65}$$

We then have for the matrix element

$$S_{1,1} = \langle 1|\psi(t)\rangle = f_1(t) = \cos(\Omega t) + i\frac{\Delta}{\Omega}\sin(\Omega t) \tag{3.66}$$

Similarly, for $S_{2,2}$ the initial conditions are $f_1(0) = 0$ and $f_2(0) = 1$. From Eqn. (3.62) we have $B = 1 - A$. So

$$f_2(t) = Ae^{i\Omega t} + (1 - A)e^{-i\Omega t} \tag{3.67}$$

Solving for $f_1(t)$

$$f_1(t) = \frac{1}{\kappa_e}\Big(- 2A\Omega\cos(\Omega t) + \Omega e^{-i\Omega t} - 2iA\Delta\sin(\Omega t) - \Delta e^{-i\Omega t}\Big) \tag{3.68}$$

The initial condition $f_1(0) = 0$ gives us

$$A = \frac{\Omega - \Delta}{2\Omega} \tag{3.69}$$

It follows that

$$S_{2,2} = \langle 2|\psi(t)\rangle = f_2(t) = \frac{\Omega - \Delta}{2\Omega}e^{i\Omega t} + \frac{\Omega + \Delta}{2\Omega}e^{-i\Omega t} = \cos(\Omega t) - i\frac{\Delta}{\Omega}\sin(\Omega t) \tag{3.70}$$

For $S_{2,1}$ the initial conditions are $f_1(0) = 1$ and $f_2(0) = 0$, the same conditions we had for $S_{1,1}$. It follows immediately that $f_2(t)$ and A are given by Eqn. (3.63) and (3.65), respectively. We have then

$$S_{2,1} = \langle 2|\psi(t)\rangle = f_2(t) = 2iA\sin(\Omega t) = 2i\Big(- \frac{\kappa_e}{2\Omega}\Big)\sin(\Omega t) = -i\frac{\kappa_e}{\Omega}\sin(\Omega t) \tag{3.71}$$

For $S_{1,2}$ the initial conditions are $f_1(0) = 0$ and $f_2(0) = 1$, the same conditions we had for $S_{2,2}$. It follows immediately that $f_1(t)$ and A are given by Eqn. (3.68) and (3.69), respectively. We have then

$$\begin{aligned}
S_{1,2} &= \langle 2|\psi(t)\rangle = f_1(t) \\
&= \frac{1}{\kappa_e}\Big(-2A\Omega\cos(\Omega t) + \Omega e^{-i\Omega t} - 2iA\Delta\sin(\Omega t) - \Delta e^{-i\Omega t}\Big) \\
&= \frac{1}{\kappa_e}\left(-2\frac{\Omega-\Delta}{2\Omega}\Omega\cos(\Omega t) + \Omega e^{-i\Omega t} - 2i\frac{\Omega-\Delta}{2\Omega}\Delta\sin(\Omega t) - \Delta e^{-i\Omega t}\right) \\
&= \frac{1}{\kappa_e}\left[-\frac{\Omega-\Delta}{2\Omega}\Omega(e^{i\Omega t}+e^{-i\Omega t}) + \Omega e^{-i\Omega t} - \frac{\Omega-\Delta}{2\Omega}\Delta(e^{i\Omega t}-e^{-i\Omega t}) - \Delta e^{-i\Omega t}\right] \\
&= \frac{1}{\kappa_e}\left[e^{i\Omega t}\left(\frac{\Delta-\Omega}{2\Omega}\Omega + \frac{\Delta-\Omega}{2\Omega}\Delta\right) + e^{-i\Omega t}\left(\frac{\Delta-\Omega}{2\Omega}\Omega + \Omega - \frac{\Delta-\Omega}{2\Omega}\Delta - \Delta\right)\right] \\
&= \frac{1}{\kappa_e}\left[e^{i\Omega t}\frac{\Delta^2-\Omega^2}{2\Omega} + e^{-i\Omega t}(\Omega-\Delta)\left(\frac{\Delta-\Omega}{2\Omega}+1\right)\right] \\
&= \frac{1}{\kappa_e}\left(e^{i\Omega t}\frac{\Delta^2-\Omega^2}{2\Omega} + e^{-i\Omega t}\frac{\Omega^2-\Delta^2}{2\Omega}\right) \\
&= \frac{1}{\kappa_e}\left(\frac{\Delta^2-\Omega^2}{2\Omega}2i\sin(\Omega t)\right) \\
&= -i\frac{\kappa_e}{\Omega}\sin(\Omega t) = S_{2,1}
\end{aligned} \tag{3.72}$$

To summarize

$$\begin{cases}
S_{1,1}(t) = \cos(\Omega t) + i\dfrac{\Delta}{\Omega}\sin(\Omega t) & (3.73)\\
S_{1,2}(t) = S_{2,1}(t) = -i\dfrac{\kappa_e}{\Omega}\sin(\Omega t) & (3.74)\\
S_{2,2}(t) = \cos(\Omega t) - i\dfrac{\Delta}{\Omega}\sin(\Omega t) & (3.75)
\end{cases}$$

Putting at $t = 0$ a single particle in state $|1\rangle$ or $|2\rangle$, the survival probability is

$$P_s(t) = |S_{1,1}|^2 = |S_{2,2}|^2 = \cos^2(\Omega t) + \frac{\Delta^2}{\Omega^2}\sin^2(\Omega t) \tag{3.76}$$

We find Rabi oscillations. Putting two particles, one in state $|1\rangle$ and the other in state $|2\rangle$, the survival probability depends on the nature of the particles. For bosons

$$\begin{aligned}
P_s^{(bos)}(t) &= |S_{1,1}S_{2,2} + S_{2,1}S_{1,2}|^2 \\
&= \left|\cos^2(\Omega t) + \frac{\Delta^2}{\Omega^2}\sin^2(\Omega t) - \frac{\kappa_e^2}{\Omega^2}\sin^2(\Omega t)\right|^2 \\
&= \left(\cos^2(\Omega t) + \frac{\Delta^2-\kappa_e^2}{\Delta^2+\kappa_e^2}\sin^2(\Omega t)\right)^2
\end{aligned} \tag{3.77}$$

For fermions

$$\begin{aligned} P_s^{(ferm)}(t) &= \left|S_{1,1}S_{2,2} - S_{2,1}S_{1,2}\right|^2 \\ &= \left|\cos^2(\Omega t) + \frac{\Delta^2}{\Omega^2}\sin^2(\Omega t) + \frac{\kappa_e^2}{\Omega^2}\sin^2(\Omega t)\right|^2 \\ &= \left(\cos^2(\Omega t) + \frac{\Delta^2+\kappa_e^2}{\Delta^2+\kappa_e^2}\sin^2(\Omega t)\right)^2 = 1 \end{aligned} \tag{3.78}$$

For distinguishable particles

$$\begin{aligned} P_s^{(dis)}(t) &= \left|S_{1,1}S_{2,2}\right|^2 + \left|S_{2,1}S_{1,2}\right|^2 \\ &= \left|\cos^2(\Omega t) + \frac{\Delta^2}{\Omega^2}\sin^2(\Omega t)\right|^2 + \left|-\frac{\kappa_e^2}{\Omega^2}\sin^2(\Omega t)\right|^2 \\ &= \cos^4(\Omega t) + \frac{\Delta^4+\kappa_e^4}{\Omega^4}\sin^4(\Omega t) + 2\frac{\Delta^2}{\Omega^2}\cos^2(\Omega t)\sin^2(\Omega t) \end{aligned} \tag{3.79}$$

We thus have Rabi-like oscillations for bosons and no evolution for fermions, being stuck in the two bound dressed states. Note that, at $\Delta = 0$, oscillations for bosons proceed at a frequency twice the value of that for the single particle case. In fact

$$\begin{aligned} P_s^{(bos)}(t;\Delta=0) &= (\cos^2(\Omega t) - \sin^2(\Omega t))^2 \\ &= (\cos(2\Omega t))^2 \end{aligned} \tag{3.80}$$

Chapter 4

Non-Hermitian photonic structures

The standard structure of quantum mechanics, as developed by Dirac and von Neumann, can be dated back to the late 1920s, and hinges on the axiom that Hamiltonians must be Hermitian operators. This ensures real eigenvalues and unitary evolution in time, thus preserving the norm of the wave function, which ultimately represents information about the state of the system, and information, in an isolated system, cannot be lost. Requiring the Hermiticity of the Hamiltonian provides us with all the correct elements to build a consistent theory which it has been shown to describe pretty well the world around us. But what happens if we flip the reasoning around and search for Hamiltonians that could give us real eigenvalues and conservation of probability, without requiring Hermiticity? In 1998 a paper by Bender and Boettcher [12] extended quantum mechanics to non-Hermitian Hamiltonians, the so-called $\mathcal{PT}$-symmetric Hamiltonians. This paper was followed by a much more refined one in 2007 [13], again by Bender.
In short, a $\mathcal{PT}$-symmetric Hamiltonian is one which is invariant under the operators $\hat{P}$ and $\hat{T}$.

$$(\hat{P}\hat{T})^{-1}\hat{H}(\hat{P}\hat{T}) = \hat{H} \tag{4.1}$$

Premultiplying by $\hat{P}\hat{T}$

$$\hat{H}(\hat{P}\hat{T}) = (\hat{P}\hat{T})\hat{H} \tag{4.2}$$

which means that $\hat{H}$ commutes with $\hat{P}\hat{T}$. The parity operator $\hat{P}$, responsible for spatial reflections, is defined through the operations $\hat{\mathbf{x}} \to -\hat{\mathbf{x}}$ and $\hat{\mathbf{p}} \to -\hat{\mathbf{p}}$, while the time reversal operator $\hat{T}$ through $\hat{\mathbf{x}} \to \hat{\mathbf{x}}$ and $\hat{\mathbf{p}} \to -\hat{\mathbf{p}}$. We can also write

$$\begin{cases} \hat{P}^{-1}\hat{\mathbf{x}}\hat{P} = -\hat{\mathbf{x}} & (4.3) \\ \hat{P}^{-1}\hat{\mathbf{p}}\hat{P} = -\hat{\mathbf{p}} & (4.4) \\ \hat{T}^{-1}\hat{\mathbf{x}}\hat{T} = \hat{\mathbf{x}} & (4.5) \\ \hat{T}^{-1}\hat{\mathbf{p}}\hat{T} = -\hat{\mathbf{p}} & (4.6) \end{cases}$$

Both parity operator and time reversal operator must preserve the canonical commutation relations, $[\hat{x}_i, \hat{p}_j]_- = i\hbar\delta_{i,j}$. In order to do so $\hat{T}$, when acted on the imaginary unit, flips its sign.

$$\hat{T}^{-1}i\hat{T} = -i \tag{4.7}$$

The operator $\hat{P}$ and $\hat{T}$ commute. It turns out that $\hat{P}$ is linear, Hermitian and unitary, while $\hat{T}$ is antilinear and antiunitary. Even though the operator $\hat{P}\hat{T}$

commutes with a $\mathcal{PT}$-symmetric Hamiltonian (by definition), they may not share a common set of eigenfunctions. This is because $\hat{P}\hat{T}$ is not a linear operator.
If every eigenfunction of a $\mathcal{PT}$-symmetric Hamiltonian is an eigenfunction of the operator $\hat{P}\hat{T}$, we say that the $\mathcal{PT}$ symmetry is *unbroken*, otherwise we say it is *broken*. $\mathcal{PT}$-symmetric Hamiltonians, in an unbroken $\mathcal{PT}$ symmetry, have real eigenvalues. It is then only a necessary condition, as it is directly shown in [13], for a system to have an unbroken $\mathcal{PT}$ symmetry, that the potential energy operator, in position representation, obeys $V(\mathbf{x}) = V^*(-\mathbf{x})$. More specifically, the potential must be even in its real part and odd in its imaginary part.
Having already established a correspondence between quantum mechanics and optics, it easy for us to build an optical structure with the correct requirements for a non-Hermitian $\mathcal{PT}$-symmetric Hamiltonian. Looking at the potential in the optical Schrödinger equation, in the weak guidance approximation, we have

$$V(\mathbf{x}) \simeq \frac{n_c - n(\mathbf{x})}{n_c} \tag{4.8}$$

We need to introduce an imaginary part for the refractive index $n(\mathbf{x}) = n_R(\mathbf{x}) + in_I(\mathbf{x})$ (with $\mathrm{Re}(n) \equiv n_R$ and $\mathrm{Im}(n) \equiv n_I$), which is associated to absorption or amplification in the material. This is done by adding suited gain and loss components to the structure. We thus need to satisfy the following conditions

$$\begin{cases} n_R(\mathbf{x}) = n_R(-\mathbf{x}) & (4.9) \\ n_I(\mathbf{x}) = -n_I(-\mathbf{x}) & (4.10) \end{cases}$$

The most simple optical structure we can build, that respects the $\mathcal{PT}$-symmetry, is shown in Figure 4.1(a). We will follow again the same conventions of Chapter 3, where time t and space z (propagation along the structure) use the same symbol, namely t, and Planck constant $\hbar = 1$. We have an infinite array of evanescently coupled waveguides with coupling rate κ between adjacent waveguides in the array and a coupling rate κ_0 between each side waveguide and the adjacent waveguide in the array. Notice that now we are calling the waveguides in the array as $|n\rangle$, with $n \in \mathbb{Z}$, and the two side waveguides $|A\rangle$ and $|B\rangle$. Waveguides $|A\rangle$ and $|B\rangle$ are coupled to waveguide $|0\rangle$ and are made of active material, with gain parameter γ_0, providing gain and loss, respectively, to the field in them. Using couple-mode theory with an exponential growth or decay for amplitudes in $|A\rangle$ and $|B\rangle$, the equations governing field amplitudes b_n, $\tilde{c}_A$ and $\tilde{c}_B$ in array waveguide $|n\rangle$ and in side waveguides $|A\rangle$ and $|B\rangle$, respectively, are

$$\begin{cases} \dfrac{db_n}{dt} = i\kappa(b_{n+1} + b_{n-1}) + i\kappa_0\tilde{c}_A e^{-i\omega_0 t}e^{\gamma_0 t}\delta_{n,0} + i\kappa_0\tilde{c}_B e^{-i\omega_0 t}e^{-\gamma_0 t}\delta_{n,0} & (4.11) \\ \dfrac{d\tilde{c}_A}{dt} = i\kappa_0 b_0 e^{i\omega_0 t}e^{\gamma_0 t} & (4.12) \\ \dfrac{d\tilde{c}_B}{dt} = i\kappa_0 b_0 e^{i\omega_0 t}e^{-\gamma_0 t} & (4.13) \end{cases}$$

where $\omega_0 = \beta - \beta_0$ is the propagation constant mismatch between side waveguide $|A\rangle$ or $|B\rangle$ and the waveguide in the array. Note that we are also including an exponential $e^{\pm\gamma_0 t}$ in the mode amplitudes for the passive waveguides in the array.

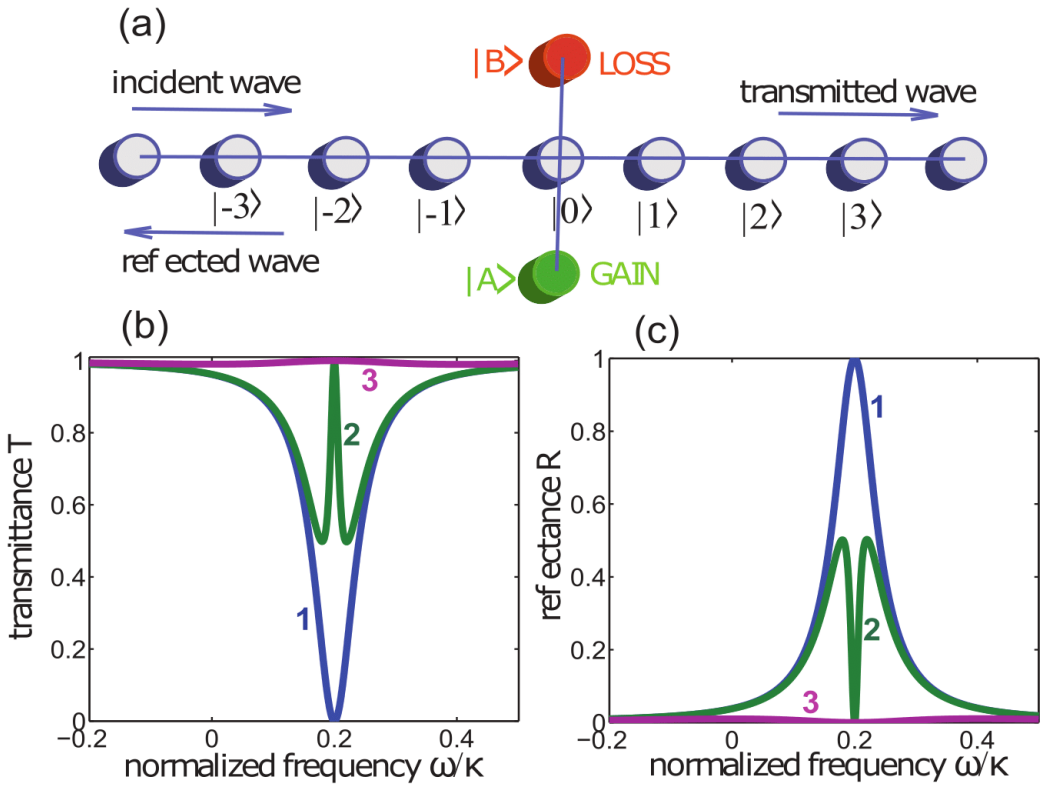

Figure 4.1: (a) Schematic of a linear infinite waveguide array and two side-coupled waveguides with optical gain and loss. (b) Spectral transmittance T and (c) reflectance R versus frequency ω of the incident wave for parameter values $\kappa_0/\kappa = 0.2$, $\omega_0/\kappa = 0.2$, and for $\gamma_0/\kappa = 0$ (curve 1), $\gamma_0/\kappa = 0.02$ (curve 2) and $\gamma_0/\kappa = 0.2$ (curve 3).

This is fine, because we are simply applying couple-mode equations (Eqn. (2.1) and (2.2)) but including these exponentials in the coupling rate between waveguides in the array and side waveguide. Define

$$\begin{cases} c_A(t) \equiv \tilde{c}_A e^{-i\omega_0 t} e^{\gamma_0 t} & (4.14) \\ c_B(t) \equiv \tilde{c}_B e^{-i\omega_0 t} e^{-\gamma_0 t} & (4.15) \end{cases}$$

Substituting in the system, we find the familiar coupled-mode equations

$$\begin{cases} i\dfrac{db_n}{dt} = -\kappa(b_{n+1} + b_{n-1}) - \kappa_0 \delta_{n,0}(c_A + c_B) & (4.16) \\ i\dfrac{dc_A}{dt} = -\kappa_0 b_0 + (\omega_0 + i\gamma_0)c_A & (4.17) \\ i\dfrac{dc_B}{dt} = -\kappa_0 b_0 + (\omega_0 - i\gamma_0)c_B & (4.18) \end{cases}$$

with an extra term due to amplification and attenuation. We know very well this structure, with its dispersion relation, $\omega(q) = -2\kappa \cos q$, where q is the Bloch wave number in the range $-\pi \leq q < \pi$. We assume an incident wave, of unit amplitude, coming from the left, so $q > 0$. Since the scattering is elastic we look for solutions of the following form

$$\begin{cases} b_n = \exp(iqn - i\omega t) + \tilde{r}(w)\exp(-iqn - i\omega t) & n \leq 0 \\ b_n = \tilde{t}(w)\exp(iqn - i\omega t) & n \geq 0 \\ c_A = A\exp(-i\omega t) \\ c_B = B\exp(-i\omega t) \end{cases} \tag{4.19}$$

where $\tilde{t}(\omega)$ and $\tilde{r}(\omega)$ are the spectral transmission and reflection coefficients for wave amplitudes (coming from the left). With this ansatz, we are just taking one component, with a specific wave number, in the usual expansion of the modal amplitude in the array (see Eqn.(2.7)). From the first two equations in the system (4.19), for $n = 0$, we get immediately that $\tilde{t} = \tilde{r} + 1$. Substituting the ansatz (4.19) into Eqns. (4.16), (4.17) and (4.18), for $n = 0$ we find

$$\begin{cases} \omega\tilde{t} = -\kappa(e^{-iq} + \tilde{r}e^{iq} + \tilde{t}e^{iq}) - \kappa_0(A + B) & (4.20) \\ \omega A = -\kappa_0\tilde{t} + (\omega_0 + i\gamma_0)A & (4.21) \\ \omega B = -\kappa_0\tilde{t} + (\omega_0 - i\gamma_0)B & (4.22) \end{cases}$$

$$\begin{cases} \omega\tilde{t} = -\kappa(e^{-iq} + \tilde{t}e^{iq} - e^{iq} + \tilde{t}e^{iq}) - \kappa_0(A + B) & (4.23) \\ A = \dfrac{\kappa_0\tilde{t}}{\omega_0 - \omega + i\gamma_0} & (4.24) \\ B = \dfrac{\kappa_0\tilde{t}}{\omega_0 - \omega - i\gamma_0} & (4.25) \end{cases}$$

Solving for $\tilde{t}$

$$\tilde{t}\omega\left(1 + \frac{2\kappa}{\omega}e^{iq} + \frac{1}{\omega}\frac{\kappa_0^2}{\omega_0 - \omega + i\gamma_0} + \frac{1}{\omega}\frac{\kappa_0^2}{\omega_0 - \omega - i\gamma_0}\right) = -\kappa e^{-iq} + \kappa e^{iq} \tag{4.26}$$

Using the dispersion relation $\frac{2\kappa}{\omega} = -\frac{1}{\cos q}$ and Euler formula

$$\tilde{t}\omega\left(1 - \frac{\cos q + i\sin q}{\cos q} + \frac{1}{\omega}\frac{2\kappa_0^2(\omega_0-\omega)}{(\omega_0-\omega)^2+\gamma_0^2}\right) = 2i\kappa\sin q \tag{4.27}$$

$$\tilde{t}\omega\left(i\frac{2\kappa}{\omega}\sin q + \frac{1}{\omega}\frac{2\kappa_0^2(\omega_0-\omega)}{(\omega_0-\omega)^2+\gamma_0^2}\right) = 2i\kappa\sin q \tag{4.28}$$

$$2i\kappa\tilde{t}\left(\sin q - i\frac{\kappa_0^2}{\kappa}\frac{\omega_0-\omega}{(\omega_0-\omega)^2+\gamma_0^2}\right) = 2i\kappa\sin q \tag{4.29}$$

Since $q > 0$ then $\sin q = \sqrt{1-\cos^2 q} = \sqrt{1-(\frac{\omega}{2\kappa})^2}$. We have

$$\tilde{t}(\omega) = \frac{\sqrt{1-(\omega/2\kappa)^2}}{\sqrt{1-(\omega/2\kappa)^2} - i\frac{\kappa_0^2}{\kappa}\frac{\omega_0-\omega}{(\omega_0-\omega)^2+\gamma_0^2}} \tag{4.30}$$

Spectral transmittance $T(\omega) = \left|\tilde{t}(\omega)\right|^2$ and reflectance $R(\omega) = |\tilde{r}(\omega)|^2$ are plotted in Figure 4.1(b) and (c) for three values of the gain parameter γ_0, with parameter values $\kappa_0/\kappa = 0.2$ and $\omega_0/\kappa = 0.2$. For $\gamma_0 = 0$ (curve 1) we see complete reflection of the wave for $\omega = \omega_0$. We have already encountered this structure, at the beginning of our discussion. The two side waveguides are separated by an even number (zero) of array waveguides, so we are expecting a Fano resonance and fractional (not complete) decay of the states $|A\rangle$ and $|B\rangle$, or no decay at all, as in this case; there is interference between decay channels, resulting in population trapping. The wave coming from the left destructively interferes with $|A\rangle$ and $|B\rangle$ and hits like a wall at $|0\rangle$, therefore bouncing back. When γ_0 is slightly increased (curve 2), but still $\gamma_0 \ll \kappa$, a transmission peak grows in the dip, reaching $T = 1$, total transmission at $\omega = \omega_0$. For strong balanced gain and loss (curve 3) every feature is washed out. This optical structure is fully analyzed in [16], including various non-linear effects. So far we have considered only linear systems where reciprocity is the rule; transmittance for waves coming from the left is the same for waves coming from the right. This is no longer true if we introduce nonlinearity. In particular Kerr-type nonlinearity, linked to the $3rd$ order electric susceptibility.
Consider the optical structure in Figure 4.2(a), having two side waveguides, $|A\rangle$ with optical gain, coupled at site $n = 0$ of the array, and $|B\rangle$ with optical loss, at site $n = N$. $\mathcal{PT}$-symmetry is preserved, but different behaviors are observed for waves coming from the left and right side. With the usual meaning of the symbols, coupled-mode equations for the modal amplitudes are easily written

$$\begin{cases} i\dfrac{db_n}{dt} = -\kappa(b_{n+1}+b_{n-1}) - \kappa_0(\delta_{n,0}c_A + \delta_{n,N}c_B) & (4.31)\\ i\dfrac{dc_A}{dt} = -\kappa_0 b_0 + (\omega_0 + i\gamma_0)c_A - \chi|c_A|^2 c_A & (4.32)\\ i\dfrac{dc_B}{dt} = -\kappa_0 b_N + (\omega_0 - i\gamma_0)c_B - \chi|c_B|^2 c_B & (4.33) \end{cases}$$

where χ measures Kerr nonlinearity in waveguides $|A\rangle$ and $|B\rangle$. Transmittance for this model can be computed numerically [17] and the results are plotted in

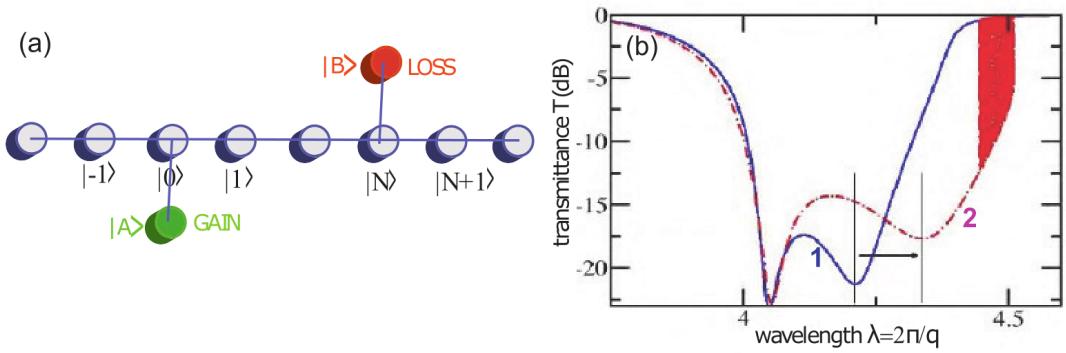

Figure 4.2: (a) Schematic of a linear infinite waveguide array and two side-coupled waveguides with optical gain and loss. (b) Numerically-computed spectral transmittance T for left (curve 2) and right (curve 1) incidence sides on a log scale. The amplitude of incident wave, for either left and right incidence sides, is set equal to one. Parameter values are: $\kappa = 1$, $\gamma_0 = 0.02$, $\omega_0 = 0$, $V = 0.5$, $N = 1$, and $\chi = 0.0125$. The wavelength is defined by $\lambda = 2\pi/q$, where q is the Bloch wave number. $\omega(q) = -2\kappa \cos q$ is the dispersion curve of the tight-binding lattice band. The shadowed area on the right of the graph, around $\lambda = 4.5$, corresponds to a bistable behavior. The horizontal arrow shows the shift of the Fano resonances due to the Kerr nonlinearity in waveguides $|A\rangle$ and $|B\rangle$. Figure (b) is adapted from [17].

Figure 4.2(b) versus inverse wave number $2\pi/q$. Both shape and position of Fano resonances are different for different directions of the incoming waves, with a red-shift for the wave coming from the gain side (curve 2) compared to the one coming from the loss side (curve 1). This non-reciprocal behavior can be exploited to build optical circuits which block light coming only from one side, known as optical isolators.

Conclusions

Fano resonance is characterized by an asymmetric lineshape of resonance profiles, which arise from the constructive and destructive interference of discrete (resonance) states with broadband (continuum) states. This phenomenon and the underlying mechanisms, being common and ubiquitous in many realms of physical sciences dealing with wave-like phenomena, can be found in a wide variety of quantum and optical systems, such as quantum dots, photonic crystals, plasmonics, and metamaterials, to mention a few.

In photonics, a simple and experimentally accessible platform to study Fano resonances is provided by light transport in arrays of evanescently coupled dielectric waveguides with defects. Scattering of discretized light by defects emulate the very basic physical origin of Fano resonances. In this master thesis we focused on some mathematical and physical aspects of Fano resonances and related phenomena in waveguide lattices: destructive interference in defect-array systems, Fano resonances and bound states in the continuum, particle statistics and Fano resonances, and Fano resonances in non-Hermitian waveguide lattices.

In photonics Fano resonance has attracted a flurry of research interest due to its asymmetric lineshape, sharp spectral features, and sensitivity to structural and environmental parameters, characteristics which make them ideal candidates for a variety of micro and nanophotonic applications such as highly-sensitive all-optical sensors. Future developments of the forefront research in the field include topological aspects of Fano resonances and bound states in the continuum, i.e. robustness arising from topological protection, and non-Hermitian Fano resonances.

Bibliography

[1] R. Douglas Gregory. *Classical mechanics*. Cambridge University Press, p. 116, 2006.

[2] U. Fano. *SULLO SPETTRO DI ASSORBIMENTO DEI GAS NOBILI PRESSO IL LIMITE DELLO SPETTRO D'ARCO*. Nuovo Cimento, 12:154-161, 1935.

[3] U. Fano. *Effects of Configuration Interaction on Intensities and Phase Shifts*. Physical Review, 124(6):1866-1878, 1961.

[4] L. W. Casperson, C. Yeh, W. P. Brown. *Scalar-wave approach for single-mode inhomogeneous fiber problems*. Applied Physics Letters, 34(7):460-462, 1979.

[5] Monika A. M. Marte, S. Stenholm. *Paraxial light and atom optics: The optical Schrödinger equation and beyond*. PHYSICAL REVIEW A, 56(4):2940-2953, 1997.

[6] A. Yariv, P. Yeh. *Photonics: Optical Electronics in Modern Communications*. Oxford University Press, 2007.

[7] S. Longhi. *Optical analogue of coherent population trapping via a continuum in optical waveguide arrays*. Journal of Modern Optics, 56(6):729-737, 2009.

[8] T. Lancaster, S. J. Blundell. *Quantum Field Theory for the Gifted Amateur*. Oxford University Press, pp. 39-41, 2014.

[9] J. Skaar, J. C. García-Escartín, H. Landro. *Quantum mechanical description of linear optics*. American Journal of Physics, 72(11):1385-1391, 2004.

[10] S. Longhi, G. Della Valle. *Many-particle quantum decay and trapping: The role of statistics and Fano resonances*. Physical Review A 86, 012112, 2012.

[11] A. Crespi, L. Sansoni, G. Della Valle, A. Ciamei, R. Ramponi, F. Sciarrino, P. Mataloni, S. Longhi, R. Osellame. *Particle Statistics Affects Quantum Decay and Fano Interference*. Physical Review Letters, 114(9):090201, 2015

[12] C. M. Bender, S. Boettcher. *Real Spectra in Non-Hermitian Hamiltonians Having $\mathcal{PT}$ Symmetry*. Physical Review Letters, 80(24):5243-5246, 1998.

[13] C. M. Bender. *Making sense of non-Hermitian Hamiltonians*. Reports on Progress in Physics 70:947-1018, 2007.

[14] S. Longhi. *Bound states in the continuum in a single-level Fano-Anderson model*. European Physical Journal B 57:45-51, 2007.

[15] S. Longhi. *Transfer of light waves in optical waveguides via a continuum*. PHYSICAL REVIEW A 78, 013815, 2008.

[16] A. E. Miroshnichenko, B. A. Malomed, Y. S. Kivshar. *Nonlinearly $\mathcal{PT}$-symmetric systems: Spontaneous symmetry breaking and transmission resonances*. Physical Review A 84, 012123, 2011.

[17] F. Nazari, N. Bender, H. Ramezani, M. K. Moravvej-Farshi, D. N. Christodoulides, T. Kottos. *Optical isolation via $\mathcal{PT}$-symmetric nonlinear Fano resonances*. Optics Express 22(8):9574-9584, 2014.

[18] A. E. Miroshnichenko, S. Flach, Y. S. Kivshar. *Fano resonances in nanoscale structures*. Reviews of Modern Physics 82:2257-2298, 2010.

[19] Y. S. Joe, A. M. Satanin, C. S. Kim *Classical analogy of Fano resonances*. Physica Scripta 74:259–266, 2006

[20] D. N. Christodoulides, F. Lederer, Y. Silberberg. *Discretizing light behaviour in linear and nonlinear waveguide lattices*. Nature 424(6950):817-823, 2003.

[21] K. Itoh, W. Watanabe, S. Nolte, C. B. Schaffer. *Ultrafast Processes for Bulk Modification of Transparent Materials*. MRS BULLETIN 31(8):620-625, 2006.

[22] A. Szameit, F. Dreisow, T. Pertsch, S. Nolte, A. Tünnermann *Control of directional evanescent coupling in fs laser written waveguides*. Optics Express 15(4):1579-1587, 2007.